AD NUMBER

ADB004610

NEW LIMITATION CHANGE

TO

Approved for public release, distribution unlimited

FROM

Distribution authorized to U.S. Gov't. agencies only; Test and Evaluation; FEB 1975. Other requests shall be referred to Air Force Avionics Lab., Wright-Patterson AFB, OH 45433.

AUTHORITY

WL/AFSC[IST] ltr, 12 Apr 1991

AFAL-TR-75-5

ADB004610

CARBON MONOXIDE GAS DYNAMIC LASER DEVELOPMENT

CALSPAN CORPORATION

TECHNICAL REPORT AFAL—TR—75—5

FEBRUARY 1975

FINAL REPORT FOR PERIOD JUNE 1973 — MAY 1974

AIR FORCE AVIONICS LABORATORY
AIR FORCE SYSTEMS COMMAND
WRIGHT—PATTERSON AIR FORCE BASE, OHIO 45433

NOTICE

When Government drawings, specifications, or other data are used for any purpose other than in connection with a definitely related Government procurement operation, the United States Government thereby incurs no responsibility nor any obligation whatsoever; and the fact that the government may have formulated, furnished, or in any way supplied the said drawings, specifications, or other data, is not to be regarded by implication or otherwise as in any manner licensing the holder or any other person or corporation, or conveying any rights or permission to manufacture, use, or sell any patented invention that may in any way be related thereto.

This technical report has been reviewed and is approved for publication.

FOR THE DIRECTOR

Ronald F. Paulson
Project Engineer

Ronald F. Paulson

Stanley E. Wagner, Chief
Electro-Optics Device Branch

Stanley E Wagner

Copies of this report should not be returned unless return is required by security considerations, contractual obligations, or notice on a specific document.

AIR FORCE/56780/4 June 1975 — 150

UNCLASSIFIED

SECURITY CLASSIFICATION OF THIS PAGE *(When Data Entered)*

REPORT DOCUMENTATION PAGE		READ INSTRUCTIONS BEFORE COMPLETING FORM
1. REPORT NUMBER AFAL-TR-75-5	2. GOVT ACCESSION NO.	3. RECIPIENT'S CATALOG NUMBER
4. TITLE *(and Subtitle)* CARBON MONOXIDE GAS DYNAMIC LASER DEVELOPMENT		5. TYPE OF REPORT & PERIOD COVERED Final Technical Report June 1973 to May 1974 6. PERFORMING ORG. REPORT NUMBER
7. AUTHOR(s) J. W. Rich, R. C. Bergman		8. CONTRACT OR GRANT NUMBER(s) F33615-73-C-1285
9. PERFORMING ORGANIZATION NAME AND ADDRESS Calspan Corporation Buffalo, New York 14221		10. PROGRAM ELEMENT, PROJECT, TASK AREA & WORK UNIT NUMBERS Project 2001 Task 01 14
11. CONTROLLING OFFICE NAME AND ADDRESS Air Force Avionics Laboratory Wright-Patterson AFB, Ohio 45433		12. REPORT DATE February 1975 13. NUMBER OF PAGES 90
14 MONITORING AGENCY NAME & ADDRESS*(if different from Controlling Office)*		15. SECURITY CLASS. *(of this report)* Unclassified 15a. DECLASSIFICATION/DOWNGRADING SCHEDULE

16. DISTRIBUTION STATEMENT *(of this Report)*

Distribution limited to U.S. Government agencies only; test and evaluation results reported; February 1975. Other requests for this document must be referred to the Air Force Avionics Laboratory (AFAL/TEO), Wright-Patterson AFB, Ohio 45433.

17. DISTRIBUTION STATEMENT *(of the abstract entered in Block 20, if different from Report)*

18 SUPPLEMENTARY NOTES

19. KEY WORDS *(Continue on reverse side if necessary and identify by block number)*

CO LASER
VIBRATIONAL ENERGY TRANSFER
VIBRATIONAL RELAXATION
GAS DYNAMIC LASERS
DIATOMIC MOLECULAR LASERS
INFRARED LASERS
INFRARED SPECTROSCOPY

20 ABSTRACT *(Continue on reverse side if necessary and identify by block number)*

The development of small, electrically excited, supersonic flow carbon monoxide lasers is reported. These lasers utilize aerodynamically stabilized, d.c., glow discharges, which have been successfully operated to pressures of 1.5 atmospheres in CO-He gas mixtures. The following performance levels have been achieved.

DD FORM 1 JAN 73 1473 EDITION OF 1 NOV 65 IS OBSOLETE

UNCLASSIFIED

SECURITY CLASSIFICATION OF THIS PAGE *(When Data Entered)*

(1) An 11 gm/sec device, operating at atmospheric discharge pressure, produces 350 watts cw at 11% efficiency, with greater than 60% of its power in the 4.8 to 5.1 micron range.

(2) A 1.5 gm/sec device, operating at discharge pressures in excess of 1.5 atmospheres, produces 17 watts cw at 4% electrical efficiency, with 90% of its power in the 4.8 to 5.1 micron range.

FOREWORD

This is the final report on work done by Calspan Corporation, Buffalo, New York, for the Air Force Avionics Laboratory (TEO), Air Force Systems Command (AFSC), under Contract No. F33615-73-C-1285, Project 2001 01 14 during the period June 1973 to May 1974. The work was monitored for the Air Force by Lt. Walter Roll and Dr. Ronald Paulson, AFAL/TEO. The report describes the results of a development program of electrically excited supersonic flow carbon monoxide lasers.

We wish to acknowledge the assistance of the following colleagues during the course of this research: Mr. J.R. Moselle and Miss M.J. Williams, who programmed the numerical calculations; Mr. E. Simme, who constructed and operated the experimental equipment; and Drs. J.W. Daiber, R.G. Rehm, and T.J. Falk for many helpful discussions.

The authors submitted this report for Air Force review on 20 July 1973. Calspan Corporation has assigned No. WG-5324-A-1 to this report.

TABLE OF CONTENTS

TABLE OF CONTENTS (Cont'd)

LIST OF ILLUSTRATIONS

LIST OF ILLUSTRATIONS (Cont'd)

LIST OF TABLES

Section I
INTRODUCTION

The present report gives the results of a one year development program for a class of electrically excited, supersonically cooled carbon monoxide lasers of novel design. These lasers use a d.c. glow discharge in the plenum of a supersonic nozzle to energize a flowing mixture of carbon monoxide and helium. The discharge selectively excites the CO vibrational mode, while the gas translational temperature remains relatively cold. The excited gas mixture is expanded to supersonic speeds in an optical cavity established transverse to the flow in the supersonic nozzle. A perspective schematic sketch of this type of CO laser is given in Figure 1. Unique features of the present design include the electric discharge, which is capable of operation at pressures of one to two atmospheres, and the very low in-cavity gas temperatures (30-40°K), which results in unusually short wavelength output for a CO laser, with the bulk of output power being in the 4.8 to 5.1 micron wavelength range. Previous reports of research and development in these laser systems are given in references 1 to 3.

The principal development goals during the past year have been:

(1) Optimization of parameters leading to high efficiency operation of moderate (100-200 watts) cw power levels in the wavelength interval of 4.8 to 6.0 microns.

(2) Development of an aerodynamically stabilized discharge which will permit operation of the laser at plenum pressures above one atmosphere.

(3) A study, design, and component test of a small scale version of the supersonic flow CO laser, leading to a device in the 50 watt cw range, with a 125 CFM pumping requirement.

The remainder of the report describes progress in the above areas during the past year. Section II discusses the development of a discharge which operates at above atmospheric pressure, and also reports parametric

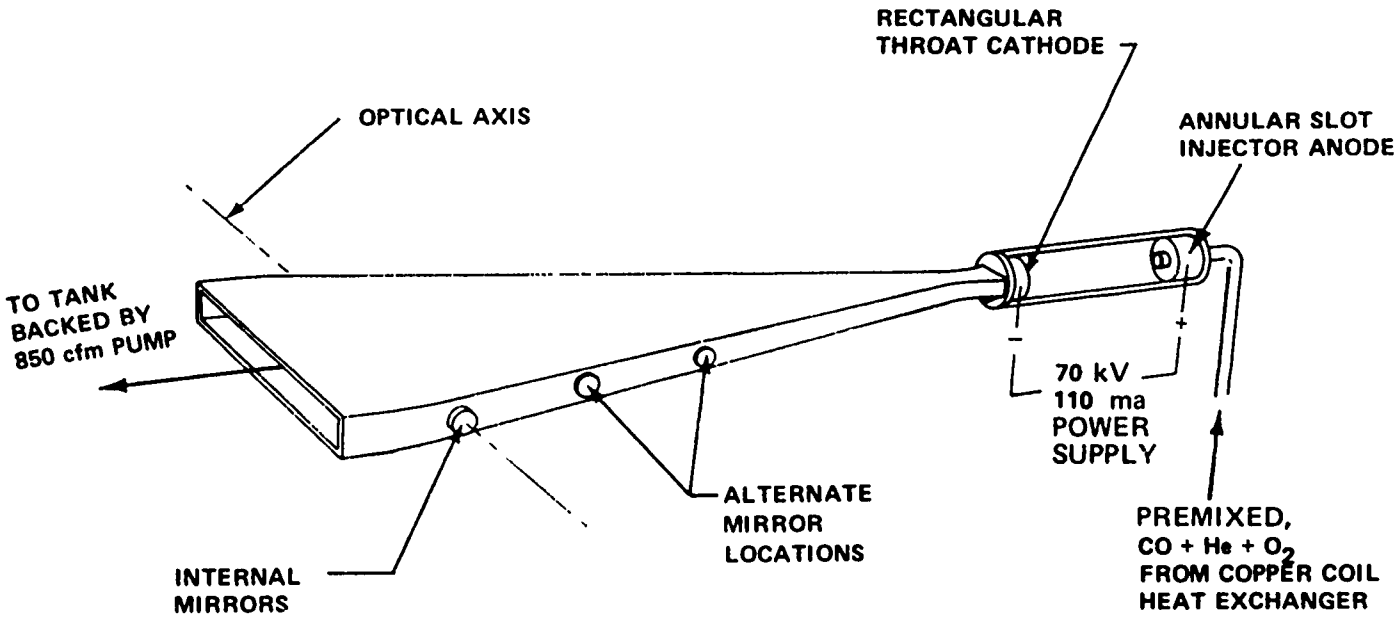

Figure 1 PERSPECTIVE SKETCH OF THE ELECTRICALLY EXCITED SUPERSONIC FLOW CO LASER

performance studies made using the improved discharge section. Section III presents a study of atmospheric attenuation of CO laser radiation. Section IV describes the conceptual design of a small scale (1.5 gm/sec) version of the laser; performance results of a prototype test are also given. The final section, V, gives a summary of results and presents conclusions and recommendations for further development.

Section II
LASER OPERATION WITH HIGH PRESSURE DISCHARGE

1. DISCHARGE DESIGN

The discharge section that has been developed provides stable glow discharge excitation of a flowing $CO/He/O_2$ plasma, at operating pressures up to two atmospheres, and electrical power loadings above 150 kw/lb/sec. The following design elements appear necessary for the stable operation of the discharge under these conditions:

i) Current-limited Power Supply

The discharge is operated from a conventional voltage-regulated d.c. power supply. However, the power supply is equipped with a saturable core reactive current limiter on the input to the primary of the supply transformer. This element prevents current being drawn from the supply above a certain preset level. During operation of the glow discharge with this power supply, if a small arc occurs, there is a tendency for the current to surge through the low-resistance path of the arc filament. Under usual conditions, this increase in current causes further ionization and rapid growth of the arc, leading to contraction of the plasma and total arc breakdown, as is well-known. However, with the current limiter, the initial current increase is limited, the rapid growth of the arc is prohibited, and the incipient arc filament generally dissipates without breakdown of the plasma. Accordingly, it is possible to operate the discharge well into the arc transition region with this method. The method offers an advantage over complete current regulation, since at the high operating voltages of these discharges, current regulation would require high voltage tubes with considerable inherent power dissipation. Finally, it should be noted that ballast resistance in series with the discharge is not required in the present system.

ii) Annular Slot Injector/Electrode

The discharge uses an aerodynamic stabilization technique first developed and used in flowing CO_2 lasers by McLeary and Gibbs.[4-6] The configuration used in the lasers under study is an axial flow glow discharge tube, 1 inch in diameter. Figure 2 gives a schematic of the discharge section. The anode is at the upstream end of the tube, and is a 1 inch I.D. copper pipe, which is adjacent to a circumferential slot through which the laser gases are injected normally to the discharge axis. The slot width is just sufficient to choke the gas flow. This method of gas injection creates a radial flow velocity component in the vicinity of the anode. As discussed in detail in Reference 4, this velocity component promotes the rapid dissipation of incipient streamwise arc filaments, and thereby increases discharge stability.

The effect of changing the polarity on the discharge electrodes was briefly examined. With the polarity reversed, the upstream electrode, adjacent to the gas injector slot, was the cathode. For operating parameters near the performance optimum, no significant effect on discharge stability or laser power and efficiency resulted. Accordingly, all data reported in the following sections are for positive polarity on the upstream electrode.

iii) Helium Diluent

Stable operation at the high power loadings and pressures quoted above has only been achieved with the use of helium as a diluent for the laser gases. Typically, from 85 to 95 percent by volume of the gas mixture is helium. As is well-known, the helium is not required for the kinetic processes which establish the population inversion in this laser.[2,7-8] The role of helium in increasing discharge stability is, apparently, to insure rapid dissipation of local arc filament "hot spots" by increasing the heat conductivity of the discharge gases. Such heat dissipation prevents growth of arc filaments and subsequent arc breakdown of the discharge.

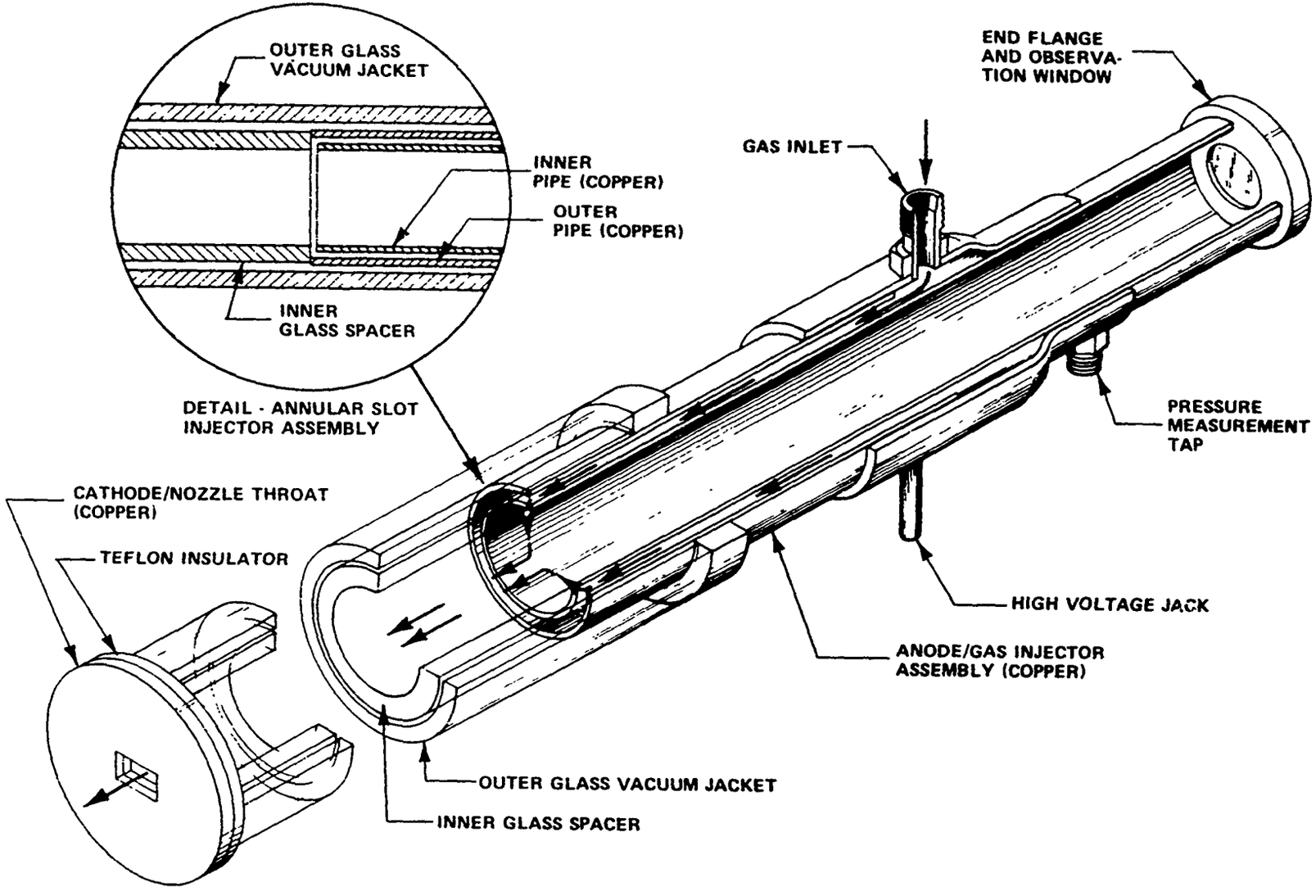

Figure 2 HIGH PRESSURE ELECTRICAL DISCHARGE CONFIGURATION

iv) Oxygen Additive

As has been observed in many electric-discharge-excited CO lasers, beginning with the work of Osgood and Eppers,[9] trace O_2 addition ($< 1\%$, see Reference 2) inhibits CO dissociation and prevents excessive carbonization of the discharge electrodes. Carbon deposits on the electrodes severely degrade performance of the laser, by causing arcing at relatively low power loadings.

v) Gas Purity

Except for specific studies of the effects of trace gas additions, the CO laser has routinely been supplied with Matheson C.P. grade carbon monoxide, certified 99.5% pure, or Linde C.P. grade carbon monoxide, certified 99.3% pure. However, the Linde supplied CO gave poorer performance levels with regard to discharge stability than the Matheson supplied gas. Further, an occasional cylinder of Matheson-supplied gas gave below-normal performance. In order to determine the cause of this variation, samples of various CO gas cylinders were submitted for gas chromatography and mass spectrometry analysis. Table 1 shows the results of these analyses for three CO gas samples. Sample 1 is from Matheson C.P. grade gas that gave good performance in the laser. Sample 2 is from a cylinder of Matheson C.P. grade gas that give unexpectedly subpar performance. Sample 3 is from a cylinder of Linde C.P. grade gas that did not give satisfactory laser performance.

It is evident from the analysis that degradation of performance with sample 2 was due to a high concentration of CO_2 impurity. The Linde supplied gas, sample 3, contained an extremely high concentration of nitrogen, plus significant amounts of hydrogen and methane.

A general conclusion of these analyses is that the purity level of the gases in this system must be $\geq 99.5\%$. This is of course not a stringent requirement on the helium, as commercial grade He greatly exceeds this purity. In the case of CO, C.P. grade gases with controlled quality should be adequate.

TABLE 1

CARBON MONOXIDE GAS ANALYSIS

	Sample 1 CP Grade 99.5% Pure Matheson CO (Satisfactory)	Sample 2 CP Grade 99.5% Pure Matheson CO (Unsatisfactory)	Sample 3 CP Grade 99.3% Pure Linde CO (Unsatisfactory)
Constituents		Concentration ppm Volume	
Nitrogen	285	240	7500
Oxygen	ND 4	ND 4	6
Argon	4	ND 4	24
Carbon Dioxide	ND 4	1360	27
Hydrogen	ND 4	ND 4	265
Heliurn	ND 10	ND 10	ND 10
Carbon Monoxide	Balance	Balance	Balance
Methane	15	ND 10	280
Total Hydrocarbons as Methane	NA	NA	NA

ND = none detected, less than

NA = not analyzed

This sample was scanned from mass 2 through mass 100 and no other constituents were detected. The detection threshold for most constituents is 4 ppm volume/volume.

Two additional elements, which are not essential for discharge stability, were also briefly investigated:

vi) Aerodynamic Baffles

An additional design element, that of aerodynamic baffles, was considered but never introduced into the discharge. These baffles were to generate a greater degree of turbulence than that provided to the inlet gases by the slot injector alone. However, due to the good discharge performance level attained without the baffles, their fabrication was not pursued. Figure 3 illustrates the proposed location of the baffles.

vii) Downstream Gas Injector

A final design consideration is also shown in Figure 3. A gas injector section is inserted in the laser downstream of the discharge section and just prior to the supersonic nozzle. Theoretical considerations suggest that the performance of the supersonic laser may be enhanced by injection of various cold gas additives through the orifice formed at this location. In this configuration the cathode is a 1 inch I.D. copper ring, 5/8 inches in length. The nozzle throat is a brass section of dimensions 1.2 x 1.1 cm. Results of tests performed using this cold gas injection system are given in Section 2.2. All the other studies discussed in this report were performed with the downstream gas injector removed.

2. LASER PERFORMANCE WITH HIGH PRESSURE DISCHARGE

2.1 Performance Without Gas Injector Section

Using the discharge design described in the preceding subsection without the gas injector section, the laser was operated at much higher discharge pressures than those obtained previously. Figure 4 gives a schematic drawing of the final laser configuration, with which all the data reported in this section were obtained. Referring to Figure 4, the premixed laser gases are introduced into the discharge section shown at the top of the drawing (Figure 2 gives a detailed schematic of this discharge section). The laser gas flows from the discharge section into the supersonic nozzle as illustrated. As discussed above, the gas injector is the anode; the discharge cathode is formed by the nozzle throat itself, which is a copper section of throat dimensions 1.2 x 1.1 cm. The nozzle is of rectangular cross section, as shown.

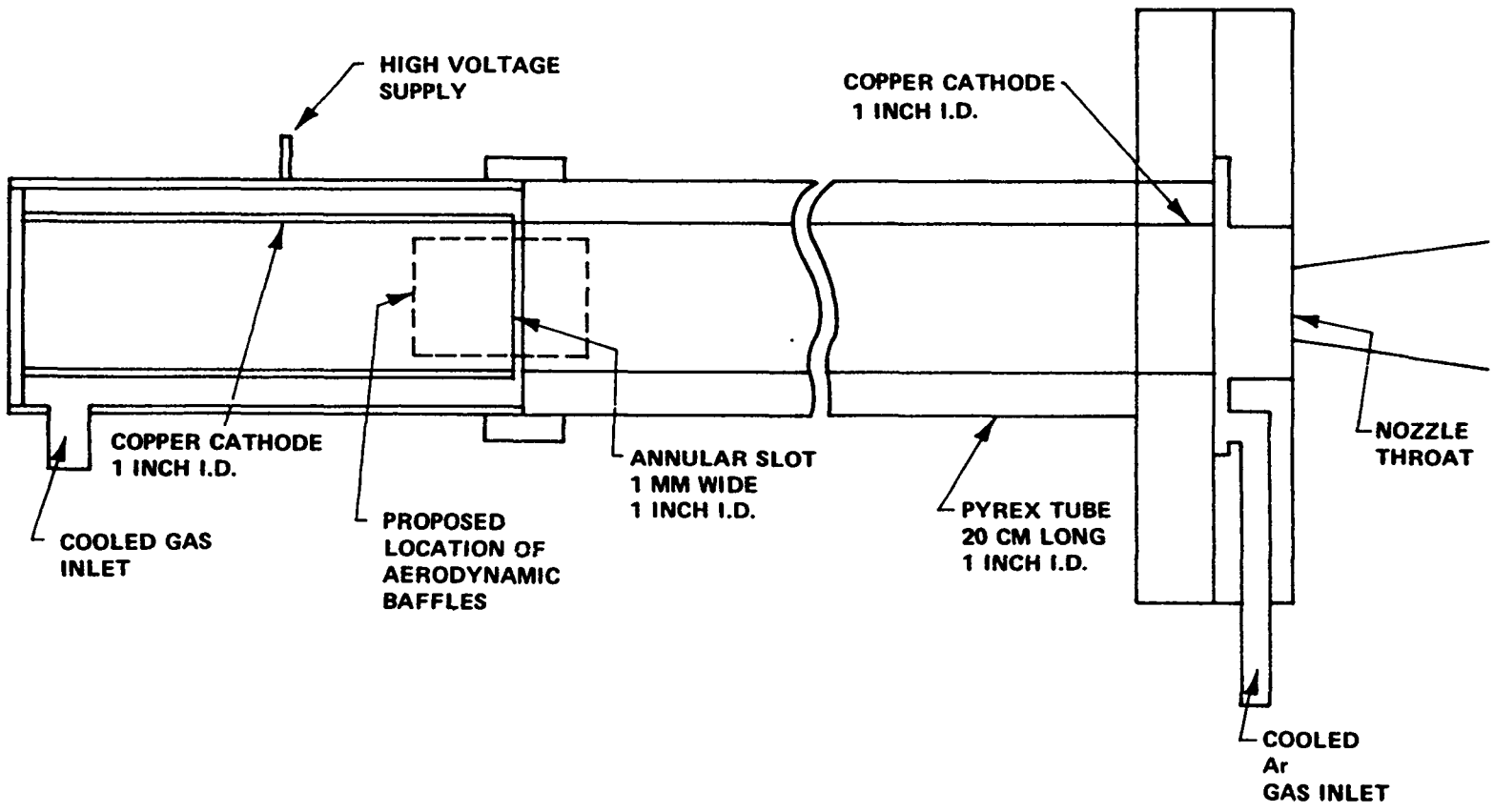

Figure 3 SLOT INJECTION AERODYNAMICALLY STABILIZED DISCHARGE CONFIGURATION

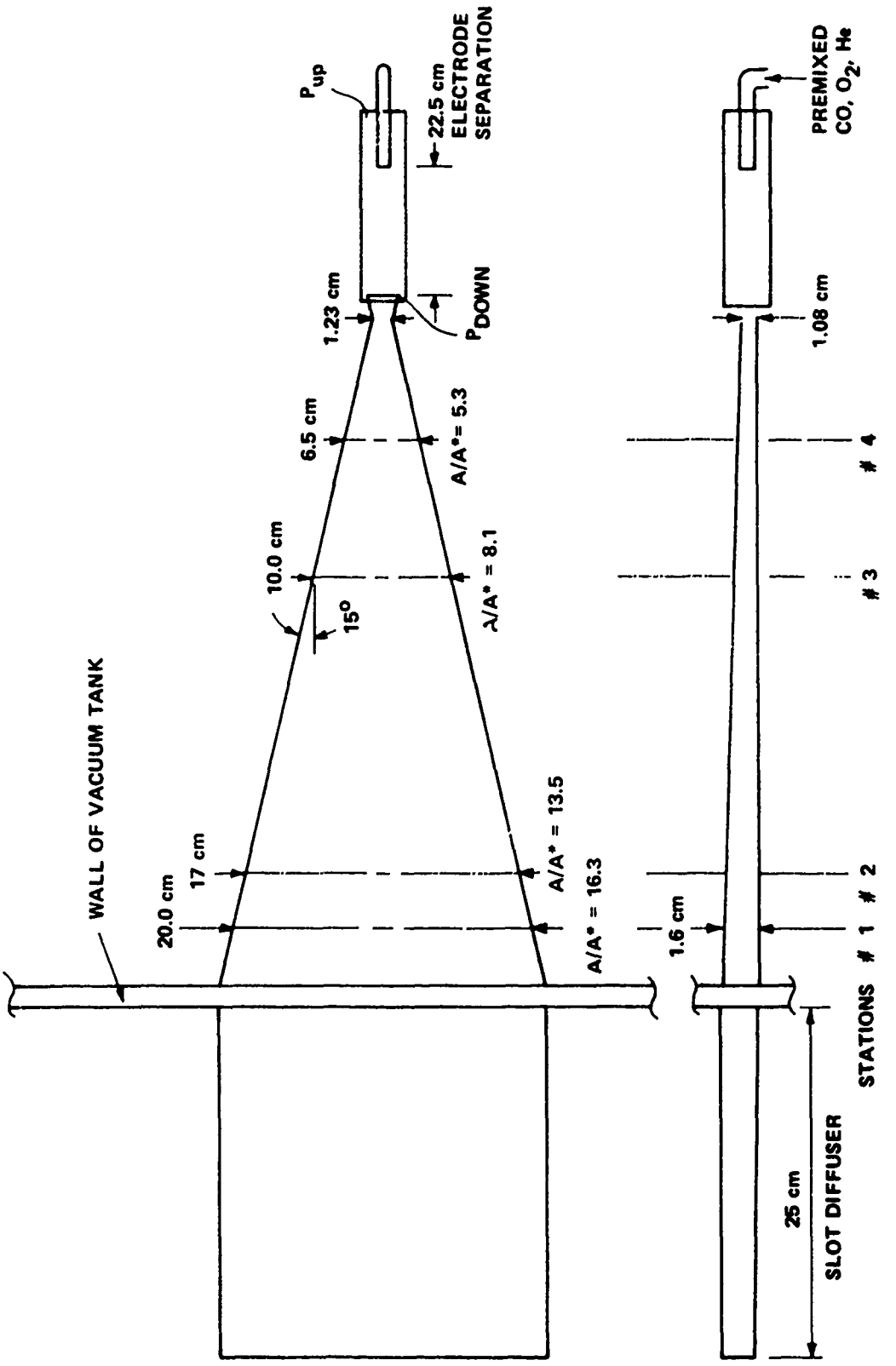

Figure 4 SCHEMATIC DIAGRAM OF THE ELECTRICALLY EXCITED SUPERSONIC FLOW CO LASER

The expansion half-angle is 15°, and the top and bottom surfaces diverge slightly to allow for boundary-layer growth. The system currently is being pumped by the Calspan flow laser facility, which consists of a 125,000 ft^3 vacuum sphere backed by 850 cfm. vacuum pumps. Use of this facility to pump the laser permits essentially continuous supersonic operation.

The optical cavity in the laser was established using a mirror system consisting of a 4 meter radius of curvature total reflector and a 15% transmitting dielectric-coated germanium flat. The mirrors were obtained commercially. The mirrors are internally mounted, recessed approximately 1 inch from the gas flow, in cylindrical mirror boxes which can be bolted in place at any of the nozzle stations shown in Figure 4. The mirror ports in the nozzle sidewalls at these stations are circular, 3/4 in. in diameter. These mirror ports are blocked with flush plugs at all stations except that selected for the optical cavity. There appears to be no major effect of the open mirror ports on the nozzle gas dynamics. Early in the program, a comparison of nozzle static pressure was made for operation with open and plugged mirror ports; no significant difference was noted. The laser data reported in this paper were all obtained with an optical cavity at the farthest downstream location in the nozzle, Station No. 1 in Figure 4.

Further details of the typical operation of this laser, information about the gas dynamic performance, and descriptions of the various diagnostic measurements which can be made during operation are given in Reference 2.

Figures 5 and 6 show typical laser performance with the high pressure discharge section. The data of these figures were obtained with a 6 inch long discharge, i.e., a 6 inch electrode separation. Also, the laser gases were entering the discharge at room temperature. Figure 5 is a plot of power output and efficiency vs. discharge current for these conditions, at a discharge pressure of 0.9 atmospheres. It can be seen that power increased steadily with discharge current to 360 watts c.w. at 90 ma. Efficiency has begun to fall off slightly at this current, maximum efficiency is 11.5% at 300 watts c.w.

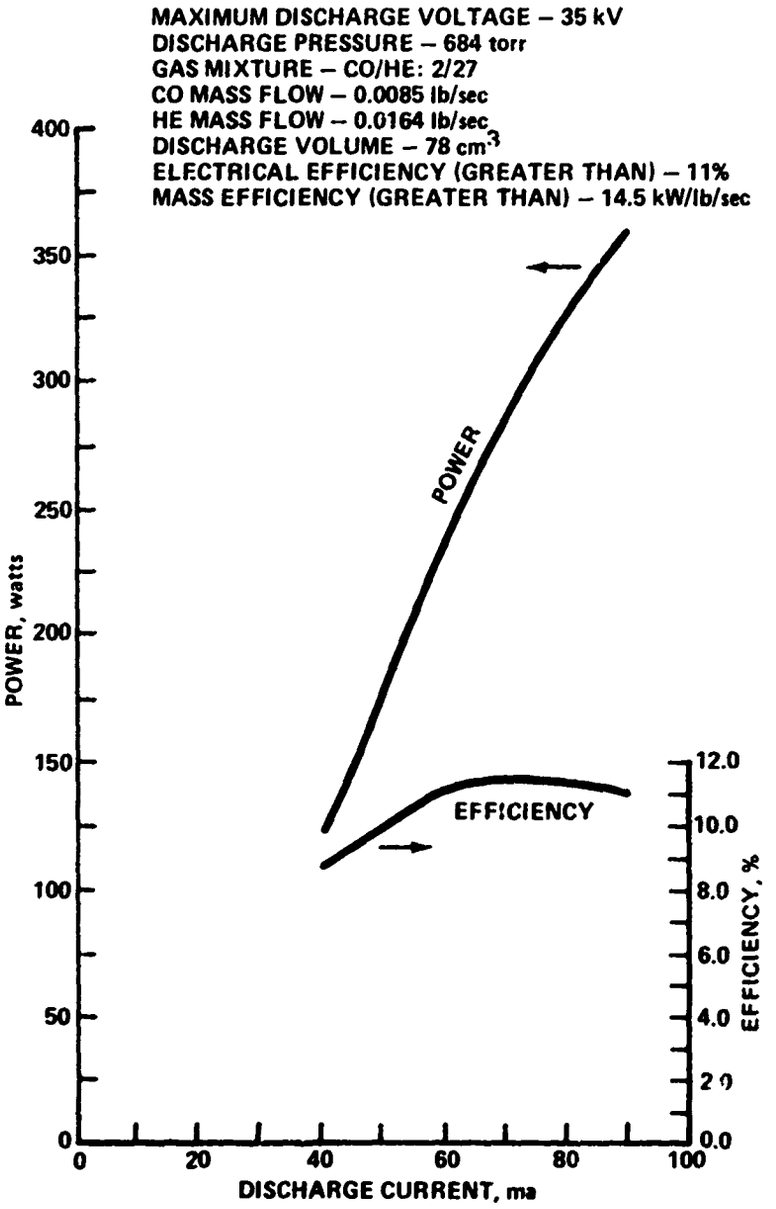

Figure 5 CO SUPERSONIC LASER PERFORMANCE AT HIGH DISCHARGE PRESSURE

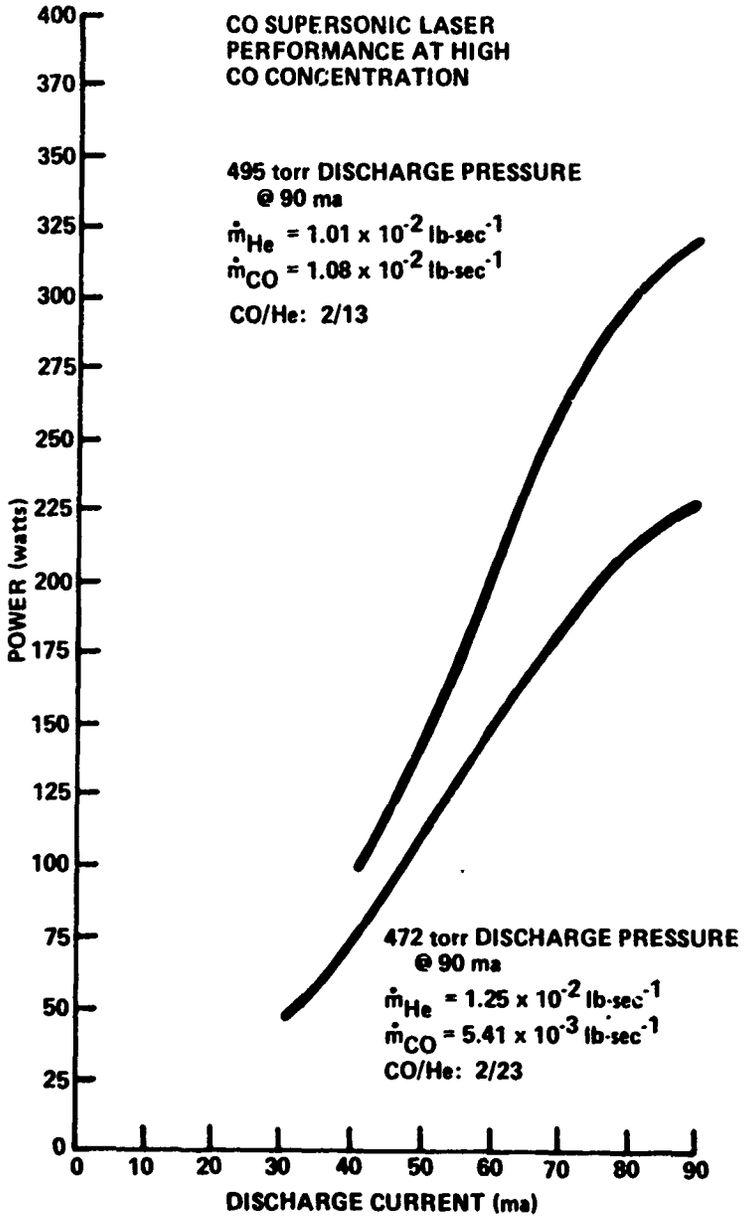

Figure 6 CO SUPERSONIC LASER PERFORMANCE AT HIGH CO CONCENTRATION

Figure 6 shows the effect of varying CO concentration. In order to strike the discharge at higher CO concentrations, it was necessary to operate at the lower total pressure of 0.65 atmospheres. As can be seen from the figure, the discharge was stable with CO concentration up to 15% and power increased with CO concentration.

Table 2 shows the results of operation of the laser at near and above atmospheric discharge pressures with varying electrode separations and inlet gas temperatures. Operation at pressures above 1.5 atmospheres was prevented by the existing gas handling system and is not a stability limit. At the 9 inch electrode separation, Run numbers 3 and 6, available voltage limited operation to one atmosphere. It can be noted that performance at the 1.5 atmosphere plenum pressure level for Run number 2, did not greatly decrease performance from the best 0.9 atmosphere results of Figure 5. Although strict comparisons can not be made between 300°K and 200°K inlet gas temperature runs, it appears that cooling of inlet gases increases electrical and mass efficiencies. It also appears that the amount of current passed through the discharge before instabilities occur decreases with the increase of electrode separation.

2.2 Performance With Gas Injector Section

Using the discharge configuration as shown in Figure 3, liquid nitrogen precooled argon was injected into the laser just prior to the nozzle throat. At the lowest argon flow rates, there was no effect on laser performance. As the flow rate was increased, laser power output decreased until at large argon flow rates laser power could be quenched almost completely. With no argon flow, laser power output was 50 watts with room temperature inlet gases and 80 watts with liquid nitrogen cooled inlet gases. These power levels are down substantially from the power levels obtained without the gas injector section installed.

The degradation of laser performance with the insertion of the gas injector section can be understood on the basis of computer model calculations. These calculations indicate that a region of subsonic flow downstream of the discharge allows significant V-T losses to occur. Due to this understanding,

TABLE 2

LASER OPERATION AT HIGH DISCHARGE PRESSURE

Run No.	Electrode Separation Inches	Pressure, Atm.	Inlet Gas Temp., °K	$\dot{m}_{He}$, lb/sec	$\dot{m}_{CO}$, lb/sec	Discharge Voltage kV	Discharge Current mA	Electrical Efficiency, %	Power, Watts	Mass Efficiency kW/lb/sec
1	3	1.5	300	.037	.005	24	160	8	285	6.8
2	6	1.5	300	.031	.007	48	70	10	350	9.2
3	9	1.0	300	.015	.008	59	60	9	320	13.9
4	3	0.9	200	.016	.011	27	115	13	400	14.8
5	6	1.1	200	.021	.007	35	75	13	350	12.5
6	9	0.8	200	.014	.005	54	50	11	300	15.8

no further gas additives, such as N_2, CO, and CO_2 were studied.

2.3 Performance With Argon Diluent

Using the discharge configuration as shown in Figure 2, the laser was operated with total replacement of the helium diluent by argon. A stable low pressure CO/Ar discharge was achieved with small concentrations of CO. However, when a small amount of N_2 was added to the CO/Ar discharge a more stable and higher pressure discharge could be maintained. In general, it was found that an N_2/Ar mixture was more stable than a CO/Ar mixture. This behavior is in agreement with the experience of the French group at C.G.E.[11] Table 3 summarizes the best performance obtained with argon diluent.

2.4 Performance With CO_2/N_2/He Discharge Mixture

Again using the configuration as shown in Figure 2, the discharge was operated with a CO_2/N_2/He mixture to compare with the high pressure performance in CO_2 recently reported by Gibbs and McLeary.[4] Table 4 gives a comparison of the discharge characteristics for the present device and the device of Reference 4. The mass flows of the present device were chosen to give a CO_2/N_2/He ratio and discharge pressure nearly equal to that in Reference 4. While both devices use an annular slot injector anode (see Section II 1.ii), the Reference 4 device uses a ring cathode compared to the rectangular throat cathode (see Section II 2.) of the present device. Further, if the gas densities of both discharges are assumed equal, then the average flow velocity of Reference 4 is 77% of the flow velocity of the present device. Finally, when arc filaments appeared in the present discharge, further power loading was ceased. In Reference 4, power loading was increased even with the formation of arc filaments.

Mirrors reflecting at 10.6 μ were installed on the nozzle at station no. 1 (see Figure 4). As expected from known kinetics data, the system did not lase. This is of course due to the fast V-T relaxation rate of CO_2 which requires a large-expansion-angle, "fast freeze" nozzle, rather than the 15° wedge presently used. It should be emphasized that the ability of the CO system to utilize high quality gas dynamic nozzles is one of the most attractive features of this CO laser, in contrast to CO_2 supersonic flow systems.

TABLE 3

ARGON DILUENT DISCHARGE CHARACTERISTICS

Ar flow rate	-	5.56×10^{-3} lb. sec^{-1}
CO flow rate	-	1.3×10^{-4} lb. sec^{-1}
N_2 flow rate	-	1.8×10^{-4} lb. sec^{-1}
Discharge Pressure	-	100 torr
Electrode Separation	-	6 inches
Discharge Current	-	80 mA
Discharge Voltage	-	12 kV
Laser Power	-	30 watts
Output Coupling	-	15%
Laser Efficiency	-	3.1%
Laser Specific Power	-	5.1 kw/lb/sec

TABLE 4

CO_2/N_2/He DISCHARGE CHARACTERISTICS COMPARED TO THOSE OF REFERENCE 4

	Present Device	Reference 4 Device
CO_2 Flow Rate	1.13×10^{-3} lb.sec^{-1}	-
N_2 Flow Rate	6.30×10^{-3} lb.sec^{-1}	-
He Flow Rate	1.46×10^{-2} lb.sec^{-1}	-
Total Mass Flow Rate	2.21×10^{-2} lb.sec^{-1}	0.869×10^{-2} lb.sec^{-1}
CO_2/N_2/He Volume Ratio	1/9/143	1/9/145
Discharge Voltage	45.7 kV	-
Discharge Current	75 mA	-
Discharge Pressure	735 torr	760 torr
Electrode Separation	9.0 inches	7.9 inches
Discharge Tube Diameter	1 inch	0.75 inches
E/N	9.53×10^{-17} volts-cm^2	9×10^{-17} volts-cm^2
Specific Power Input	155 kw/lb/sec	226 kw/lb/sec

2.5 Selected Wavelength Operation

Calculations were performed to estimate requirements for operating the supersonic flow laser in the wavelength selective mode. Two approaches were considered: 1) the use of an optical grating in place of one cavity mirror, and 2) the use of an intra-cavity water vapor cell. The optical grating would give single line lasing; the water vapor cell would only force multi-band lasing on lines having relatively low atmospheric attenuation coefficients.

The calculations indicated that either of the above approaches required the introduction of external optics in the laser. In the case of a 300 line/mm optical grating, a 30" mirror separation would be required to separate adjacent vibrational-rotational lines. In the case of a water vapor cell, comparable lengths would be required unless pressurized steam were used in the cell. Accordingly, the laser was modified with the installation of a Brewster's angle CaF_2 window in place of the output coupling mirror's internal mount. Further, external optics were set up, including a circulating water, edge-cooled mirror mount, and an optical grating mount.

However, operation with the external mirror mount greatly reduced the amplitude stability of the laser power output. As an example, with the laser operating at the 160 watt level, amplitude fluctuations of $\pm$ 10% occurred in a few seconds time scale. It appeared that improved amplitude stability with the external optics would require better control on the length of the optical cavity. It was not possible to modify the optical arrangement to accomplish this control during the time available in the present program. Accordingly, further wavelength selective studies were not performed in this period.

2.6 Beam Quality and Beam Divergence

With the optical cavity of the supersonic laser in the external configuration, as discussed in the previous subsection, an aperture was positioned in the cavity to study its effect on beam divergence. Near-field burn patterns in a cooled plexiglass block obtained at several distances, up to 12 feet from the output mirror, were used to determine the beam divergence.

Table 5 presents a comparison of three optical configurations. Case 1 is an internal mirror case where the aperture diameter of 0.75 inches is

TABLE 5

Beam Divergence Survey

Case	Output Coupling Mirror	Total Reflectorr Mirror	Mirror Separation, Inches	Aperture Dia. Inches	Spot Dimensions,[1] Inches	Divergence, Milliradians
1	15% flat internal	4 m rad. curv., internal	11	0.75	Rectangular, .22 x .51[2]	4.7[3]
2	15% flat external	4 m rad. curv., internal	21	0.75	Rectangular, .22 x .51[4]	1.3
3	15% flat external	4 m rad. curv., internal	21	0.50	Circular, .30 dia.	1.2

1 At output mirror.

2 Burn pattern remains rectangular to at least 150" from output mirror.

3 Divergence in plane of flow direction. Divergence normal to flow plane is smaller.

4 Burn pattern becomes roughly circular at distances greater than 2 feet from output mirror. Side lobes are evident.

formed by the opening in the nozzle wall. Beam divergence is 4.7 milliradians with a rectangular burn pattern from the output mirror to a distance of 150 inches. Case 2 is an external mirror case where again the aperture is formed by the nozzle wall opening, but the cavity length is increased 10 inches. Beam divergence is reduced to 1.3 milliradians with a rectangular burn pattern to approximately 2 feet from the output mirror and then a roughly circular pattern with side lobes to 150 inches. Case 3 is an external mirror case where a 0.50 inch diameter aperture is placed in the cavity, 2.5 inches from the output mirror. Beam divergence is 1.2 milliradians with a circular, but still highly multimode, burn pattern.

Section III
ATMOSPHERIC ATTENUATION STUDY

The attenuation of the output of the supersonic laser, due to molecular absorption in the atmosphere, was calculated. The attenuation coefficients calculated by McClatchey [10] were used.

The fractional atmospheric transmission (T) of the laser beam through a given distance (ℓ) was calculated from

$$T \equiv \frac{I}{I_o} = \frac{\sum_{V,J} P(V,J)\, e^{-k(V,J)\,\ell}}{\sum_{V,J} P(V,J)} ,$$

where I_o is the total beam power emitted by the laser, I is the beam power transmitted through a distance ℓ, P(V, J) is the power emitted by the laser on a single vibrational-rotational line, and V, J are the vibrational and rotational quantum numbers for the upper laser level of the line. The attenuation coefficients, $k(V, J)$, are taken from Reference 10. T was calculated for the data reported for the supersonic flow CO laser in Tables I-VIII of Reference 2. Figure 7 shows T plotted against path length in kilometers for the laser operating with precooled (~200°K) gases entering the discharge. Figure 8 is a similar plot for the laser operating with room temperature gases. Finally, Figure 9 shows a comparison of the best cases from Figures 7 and 8 with the fractional atmospheric transmission of a conventional liquid-nitrogen wall-cooled CO laser. The conventional laser data were obtained from previous Calspan work, Table II of Reference 12. The very great advantage of the supersonic flow CO laser over the conventional system in regard to atmospheric transmission is evident. For example, more than 20% of the supersonic flow beam can be transmitted through 5 kilometers, wheras less than 2% of the conventional laser beam is transmitted.

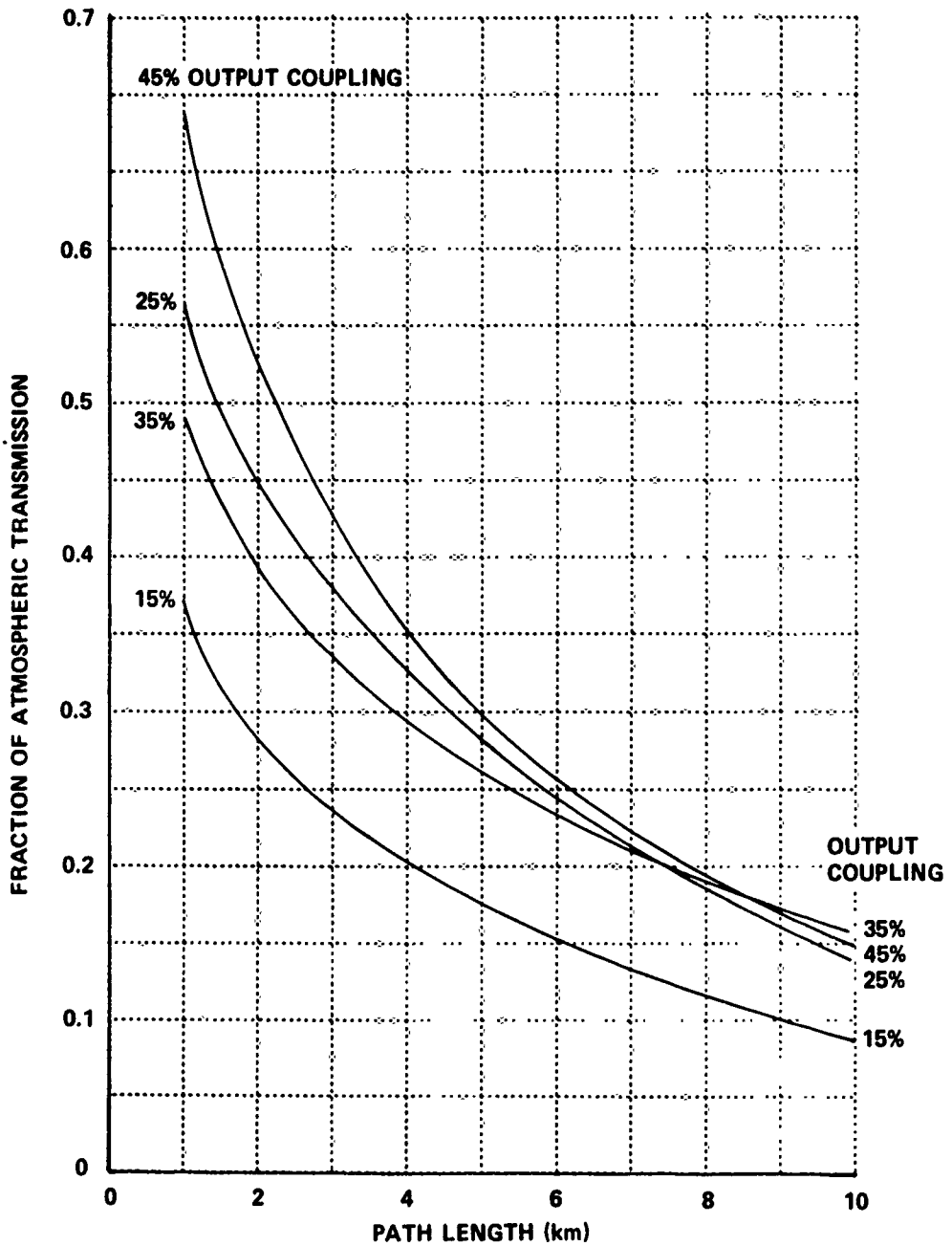

Figure 7 ATMOSPHERIC TRANSMISSION OF CO RADIATION, PRECOOLED OPERATION

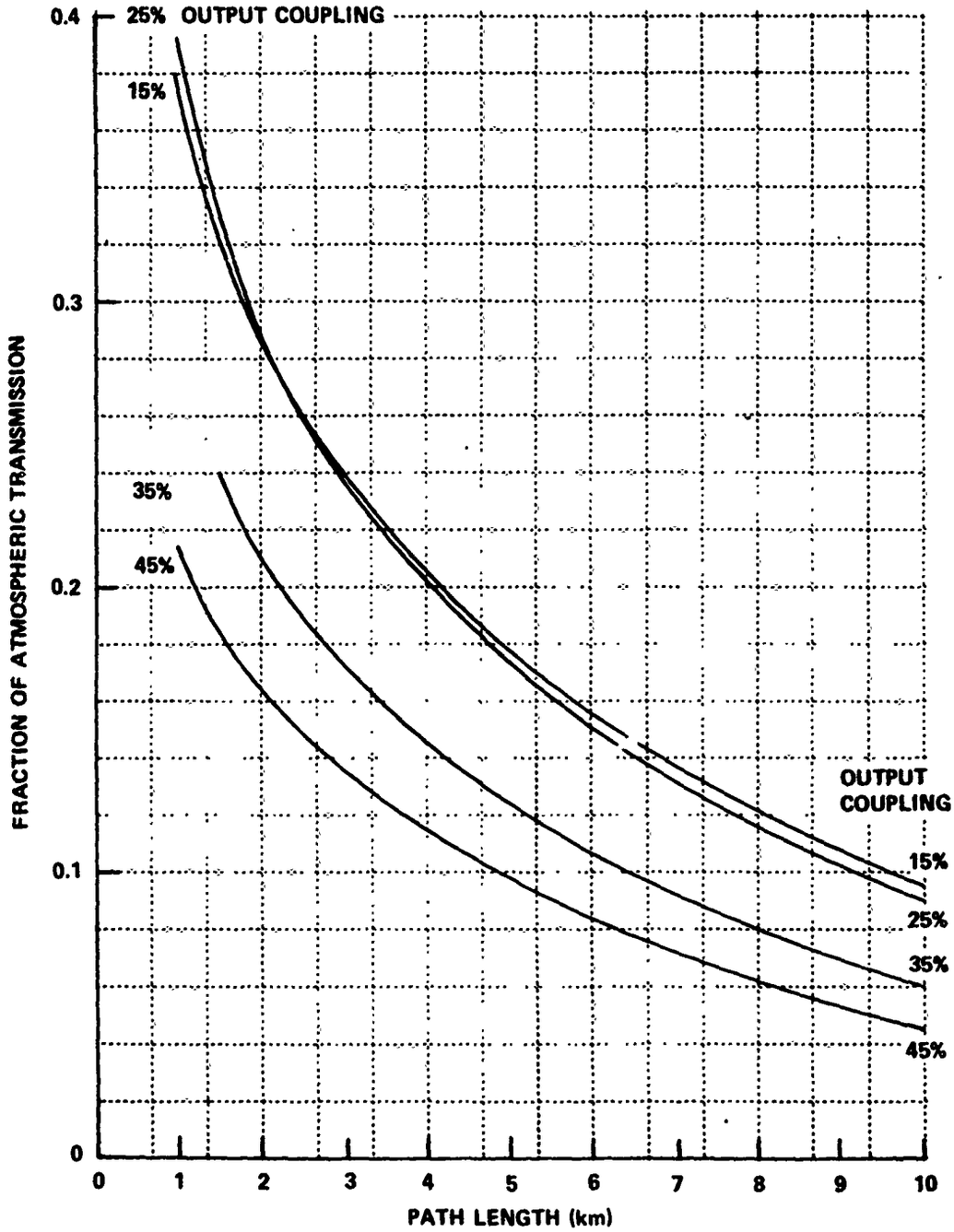

Figure 8 ATMOSPHERIC TRANSMISSION OF CO RADIATION, ROOM TEMPERATURE OPERATION

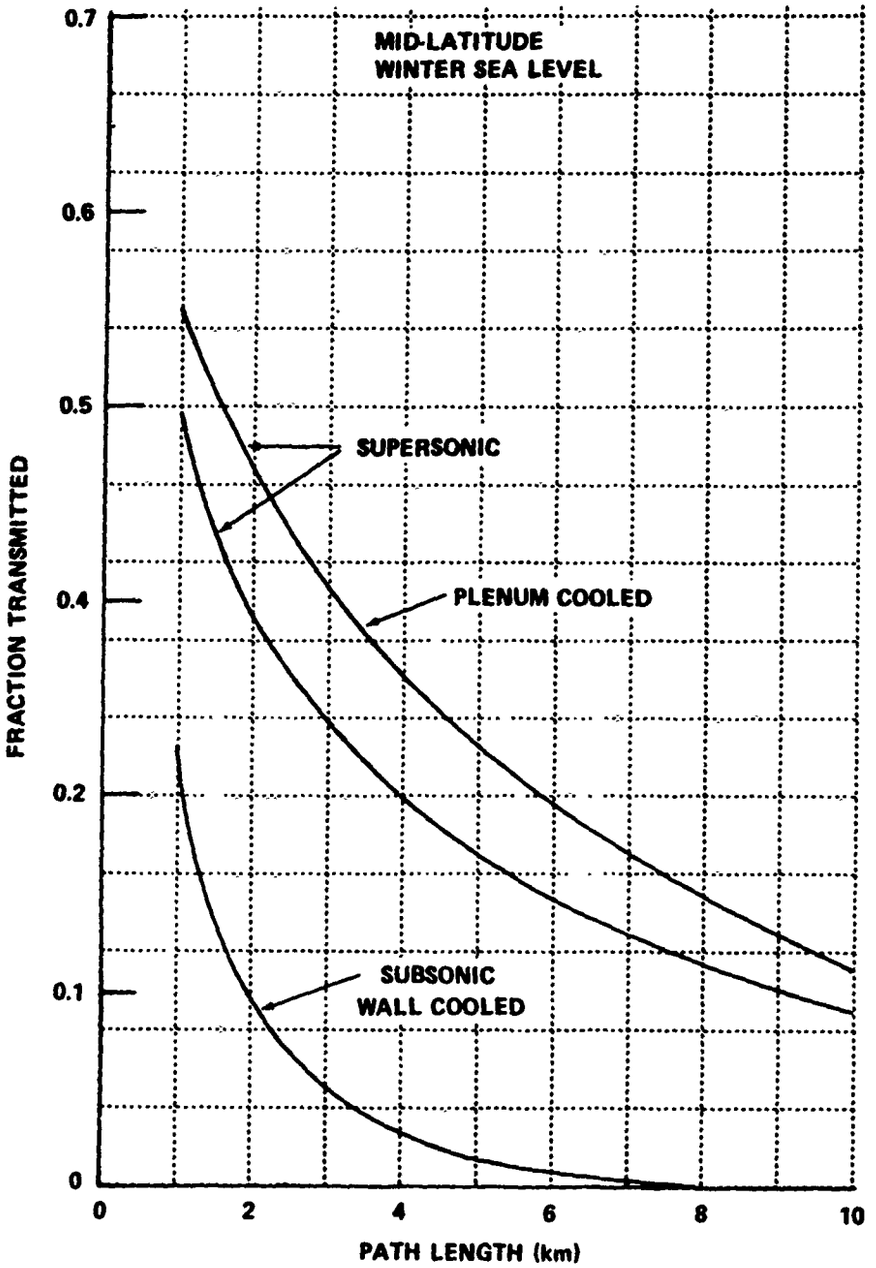

Figure 9 CO LASER PROPAGATION

Section IV
SMALL SCALE LASER DESIGN AND OPERATION

1. DESIGN CONSIDERATIONS

The laser discussed in the previous section (II) of this report is a device with mass flows in the range 12-15 gm/sec and output powers ranging to 350 watts c.w. and higher. In the present section, progress is reported in the development of a small scale version of this laser. The device discussed in the present section has mass flows of typically 1.5 gm/sec range, and is designed for power levels in the 20-50 watt c.w. range. As discussed below, pumping requirements would be in the 100-150 cfm range and a complete system would be feasible for packaging in an avionics pod. Figure 10 shows a sketch of such a system. The laser uses a glow discharge tube, 1/2 inch diameter and 2 inches length. Premixed CO and He gases are introduced into the upstream end of the tube. After the gases are excited by the discharge, they are expanded in a small supersonic nozzle, which is approximately 4 inches long. Mirrors are placed at the downstream end of the nozzle, to establish an optical cavity transverse to the flow. Continuous supersonic flow is maintained in the optical cavity by a 125 cfm pump, attached to the laser via a straight section downstream of the nozzle. The following subsections outline some of the design details of these components.

1.1 Electric Discharge Characteristics

Table 6 gives a summary of the design operating conditions for the discharge. Gases are injected into the laser through annular injector orifices, as shown. The pressure ratio across the annular injectors is such that the orifices are operated under fluid mechanically choked conditions. The injector section also serves as the anode. The cathode plate is located 5.2 cm downstream of the injector/anode section. In the center of the cathode is a 0.25 x 0.50 cm rectangular opening, which serves as the nozzle throat.

As indicated in the table, the discharge is to be operated at a 1.5 atmosphere gas pressure, and powered by a 1.5 kilowatt D.C. supply,

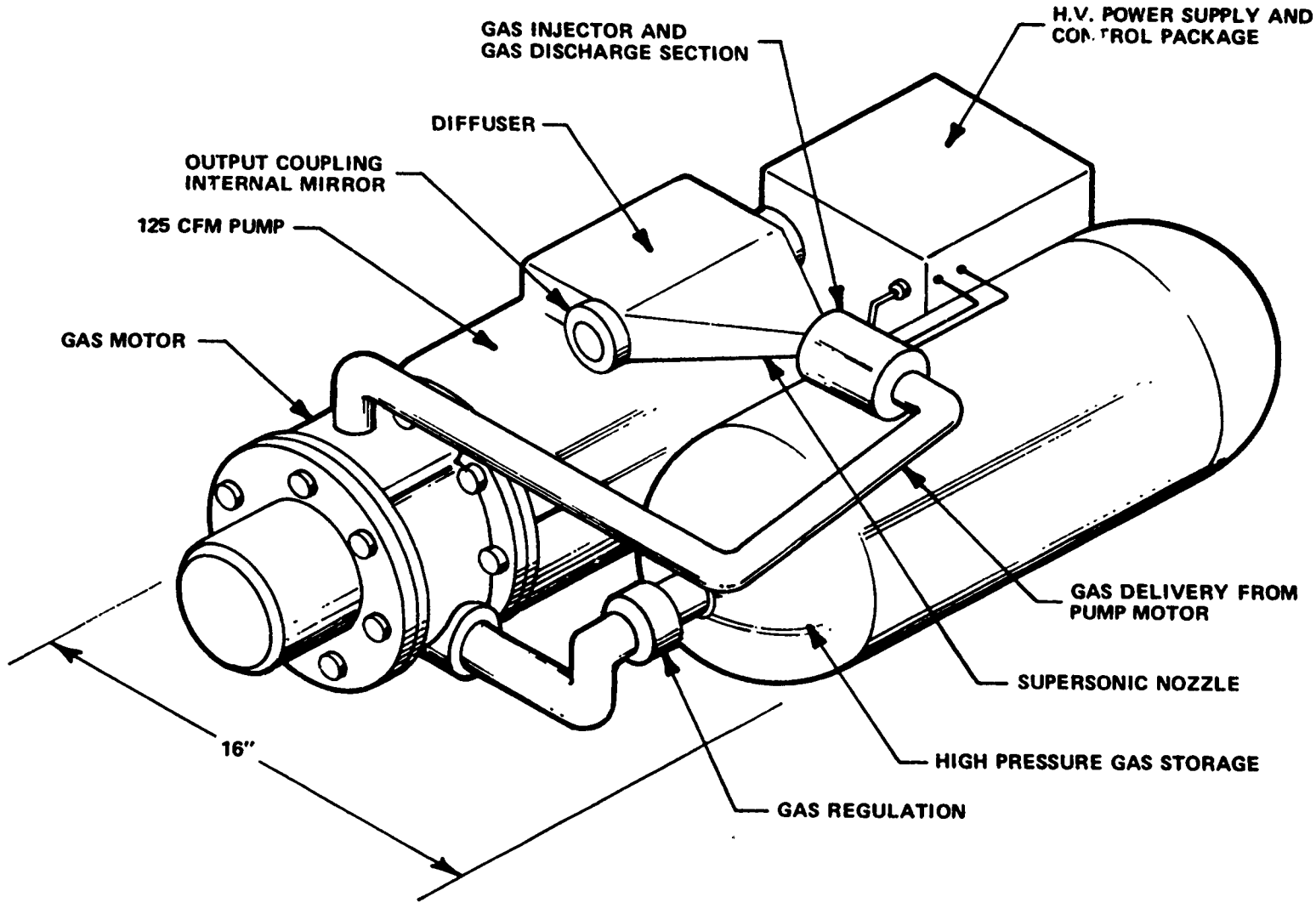

Figure 10 SMALL SCALE CO SUPERSONIC LASER SYSTEM

TABLE 6

SMALL SCALE ELECTRIC DISCHARGE CHARACTERISTICS

Input Power	-	1.5 kw
Voltage	-	20 kv
Current	-	75 ma
Electrode Separation	-	5.2 cm
Tube Diameter	-	1.3 cm
Gas Mixture	-	95.6% He, 4.4% CO by volume
Operating Pressure	-	1.5 atmospheres
Mass Flow Rate	-	1.66 gm/sec

operating at 20 kv/75 ma. Operating experience with discharges of this design indicates that only a saturable reactor current limiter is required for stable operation; current regulation or large resistive ballasting are not necessary.

Calculations of the performance of the design discharge have been performed using the Calspan CO discharge kinetics codes. The predictions of these codes previously have been correlated with the performance of the larger laser described in Section II above. Figure 11 shows variation of temperature and vibrational energy through the discharge. In the present design, maximum efficiency of vibrational model excitation has been sacrificed to obtain small size and greatly reduced pump requirements.

1.2 Supersonic Nozzle and Optical Cavity Characteristics

The nozzle is a 15° half angle wedge, with throat dimensions 0.50 x 0.25 cm. The top and bottom surfaces diverge slightly to compensate for boundary layer displacement. Dimensions and gas dynamic characteristics of the nozzle are given in Table 7.

Calculations have been performed for transverse optical cavities located at either of two downstream stations: 5 cm from the nozzle throat, and 9 cm from the nozzle throat. These distances correspond to ratios of the channel cross-sectional area to the throat area of $A/A_{throat} = 6$ and $A/A_{throat} = 10$, respectively. The expansion ratios give in-cavity Mach numbers of M = 4 and M = 5. The system can be built with either cavity location; the choice can be determined by the power and spectral output requirements of the application. The optical cavity would be formed by two internal mirrors, one totally reflecting and one 5% transmitting to provide output coupling. Beam size, without aperturing or additional optics, is approximately 0.2 x 0.8 cm. Figure 12 gives the predicted spectral distribution of the laser output, and Table 8 lists the wavelengths and quantum state assignments for the predicted maximum gain spectral lines. Table 8 also gives the atmospheric propagation coefficients calculated for these lines by McClatchey,[10] where these are available. Propagation coefficients are listed for both sea level and 5-6 km altitude.

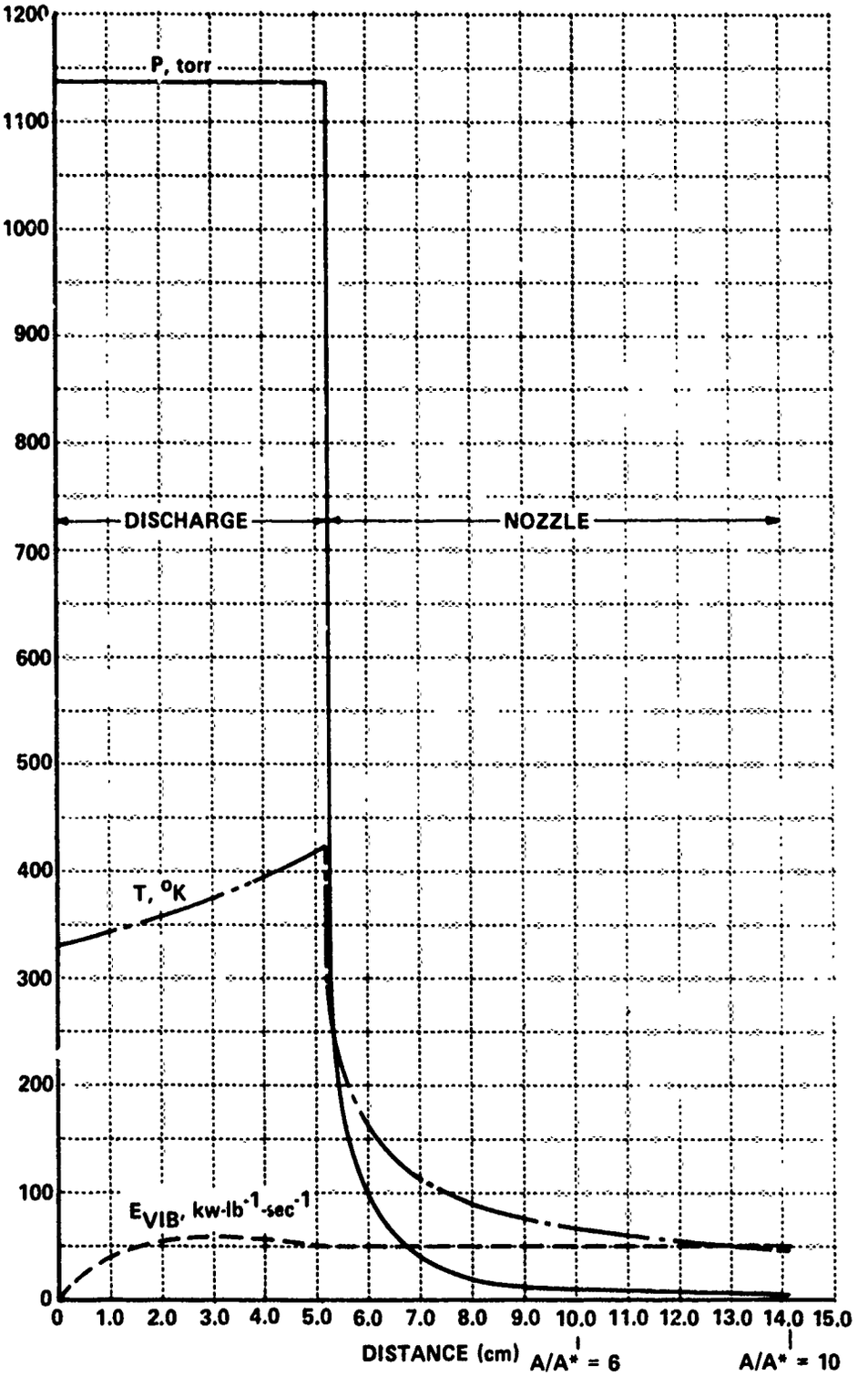

Figure 11 PRESSURE, TEMPERATURE, AND VIBRATIONAL ENERGY IN THE SMALL SCALE CO LASER

TABLE 7

SMALL SCALE NOZZLE CHARACTERISTICS

Throat Size: .25 x .5 cm

Divergence Half Angle: 15°

A/A_{throat}	Static Pressure, Torr	Mach No.	Velocity, cm/sec	Normal Shock Recovery Pressure, Torr	Volumetric Flow Rate After Normal Shock Recovery, cfm.
6	6.4	4	1.7×10^5	272	82
10	4.0	5	1.8×10^5	160	133

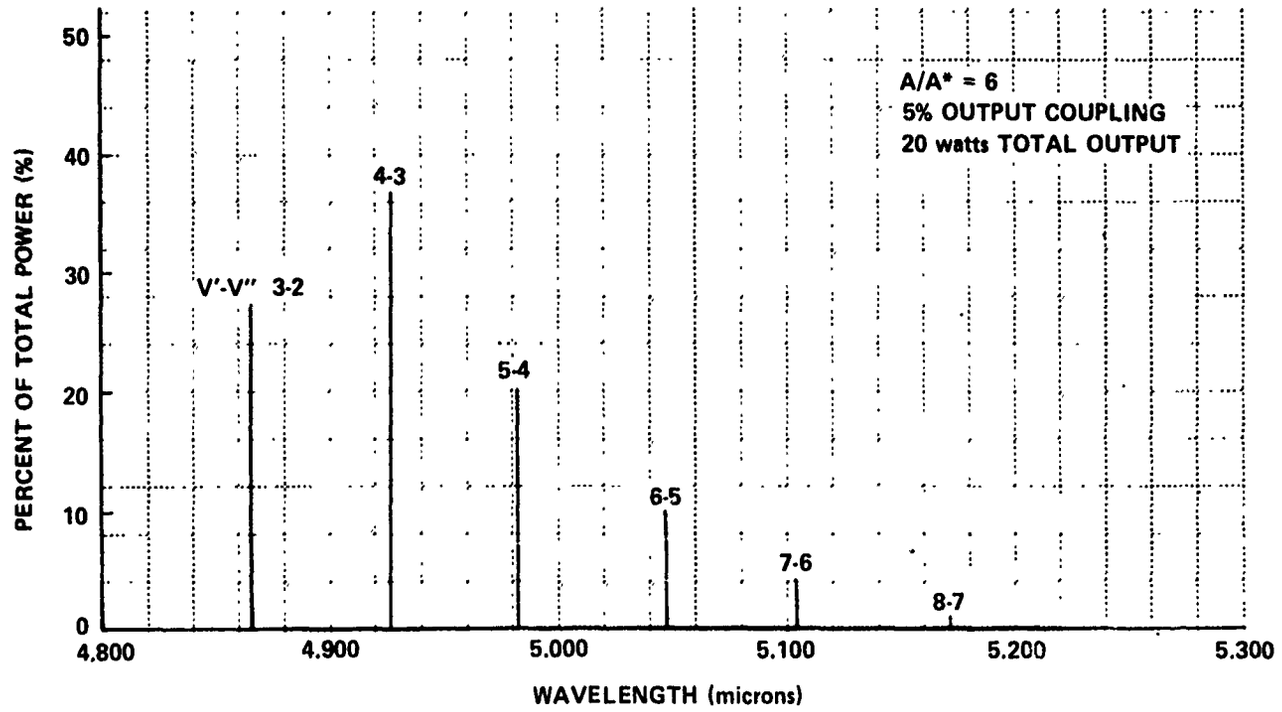

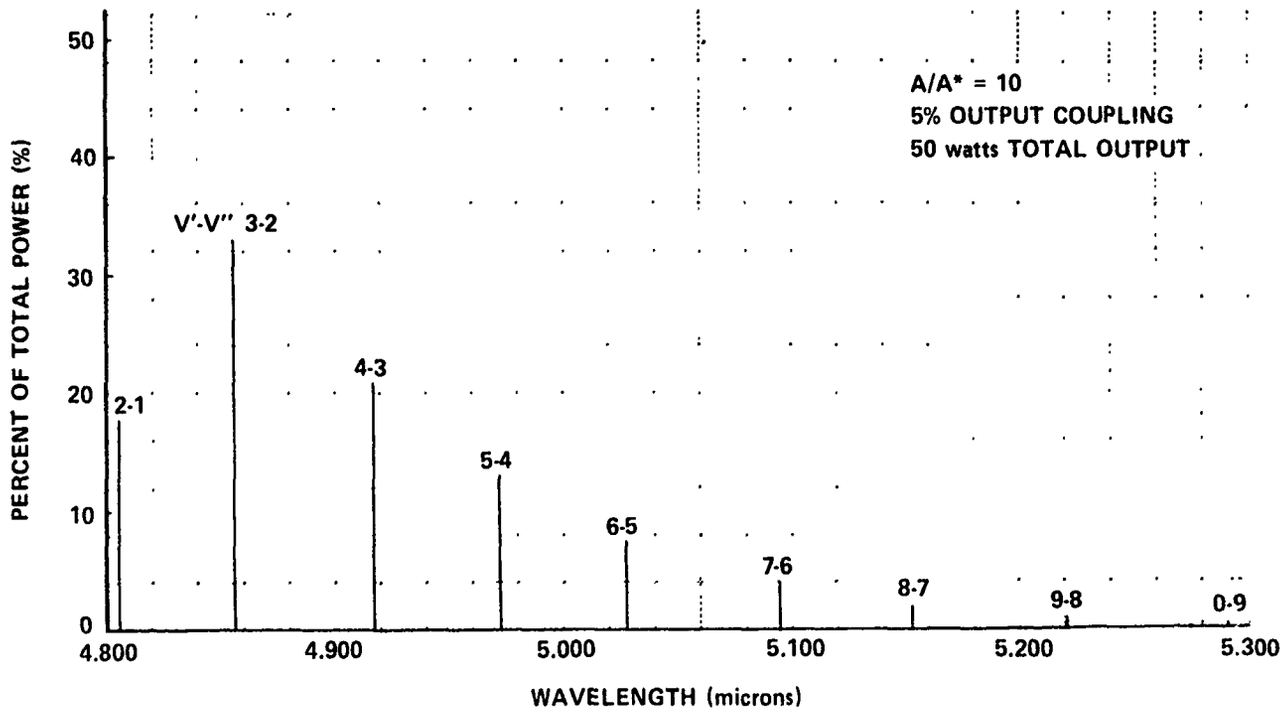

Figure 12 SPECTRAL DISTRIBUTIONS OF SMALL SCALE LASER OUTPUT

TABLE 8

SMALL SCALE LASER SPECTRAL LINE IDENTIFICATION
AND ATMOSPHERIC TRANSMISSION DATA

Cavity at A/A* = 6; 5% Output Coupling

Vibrational Band	Rotational Line	Wavelength, Microns	Attenuation Coefficients, (Km^{-1}) Mid-Latitude Winter 0 Km	5-6 Km
3-2	8	4.85624	0.0973	0.005980
	9	4.86581	0.347	0.2645
	10	4.87549	0.0623	0.006523
4-3	8	4.91849	0.0215	0.0006335
	9	4.92822	0.0284	0.001161
	10	4.93808	0.0708	0.002459
5-4	7	4.97242	0.138	0.008990
	8	4.98220	0.225	0.006833
	9	4.99209	0.0502	0.001583
6-5	7	5.03745	0.108	0.003364
	8	5.04739	0.119	0.002939
	9	5.05746	0.0737	0.002696
7-6	6	5.09401	*	*
	7	5.10400	*	*
	8	5.11412	*	*
8-7	6	5.16198	*	*
	7	5.17214	*	*
	8	5.18245	*	*

*Data Unavailable

TABLE 8 (cont'd).

Cavity at $A/A^* = 10$; 5% Output Coupling

Vibrational Band	Rotational Line	Wavelength, Microns	Attenuation Coefficients, (Km^{-1}) Mid-Latitude Winter 0 Km	5-6 Km
2-1	8	4.79538	*	*
	9	4.80479	*	*
	10	4.81432	*	*
3-2	7	4.84679	0.139	0.01024
	8	4.85624	0.0973	0.00598
	9	4.86581	0.347	0.2645
4-3	7	4.90888	0.0802	0.006209
	8	4.91849	0.0215	0.0006335
	9	4.92822	0.0284	0.001161
5-4	6	4.96277	0.229	0.007127
	7	4.97242	0.138	0.008990
	8	4.98220	0.225	0.006833
6-5	5	5.01793	7.40	0.2410
	6	5.02763	1.91	0.05713
	7	5.03745	0.108	0.003364
7-6	5	5.08415	*	*
	6	5.09401	*	*
	7	5.10400	*	*
8-7	4	5.14205	*	*
	5	5.15195	*	*
	6	5.16198	*	*
9-8	4	5.21129	*	*
	5	5.22137	*	*
	6	5.23158	*	*
10-9	4	5.28222	*	*
	5	5.29247	*	*
	6	5.30286	*	*

*Data Unavailable

It should be emphasized that many of the lines predicted for this small scale supersonic CO laser system compare favorably with CO_2 atmosphere propagation. The short wavelength lines of this laser are quite different from the output of more conventional, wall cooled CO lasers. Such systems emit peak power on lines having relatively poor atmospheric propagation characteristics.

As noted in Figure 12, the total beam bower predicted for the A/A_{throat} = 6 cavity is 20 watts, while that predicted for the A/A_{throat} = 10 cavity is ~50 watts. However, the A/A_{throat} = 6 beam does appear to offer somewhat better atmospheric transmission properties over the A/A_{throat} = 10 beam, as can be seen from a comparison of the attenuation coefficients in Table 8. In addition, operation at lower area ratios is desirable in that shock-wave-induced medium inhomgeneities are less severe at the lower Mach numbers associated with lower area ratio expansions.

1.3 Associated Systems

1.3.1 Diffuser and Pump

The diffuser section is designed for three purposes:

(i) To prevent flow separation in the optical cavity

(ii) To obtain normal shock recovery conditions at the pump inlet.

(iii) To provide a transition section into the pump.

For this purpose, the diffuser section is designed to gradually reduce the divergence of the flow channel, terminating in a straight section joined to the pump. Table 7 gives gas flow conditions entering the pump.

The recommended pump for this system is a 125 cfm sliding vane rotary pump. Weight of off-the-shelf commercial units is 180 lbs.; however, light-weight systems can be made within the state-of-the-art for less than 100 lbs.

Pump power required is approximately 5 kw, with a shaft rpm of 2000. While an electrical motor could be used to supply this power, a more desirable method for the pump discussed above is to use another rotary vane unit, this unit to be driven by the compressed laser gas supply and run as a motor. This will be a six horsepower unit, and of considerably less weight than the pump. Off-the-shelf equipment, as supplied, for instance, by Gast Corporation, would weigh 69 lbs.; a specially-built motor would weigh less than 50 lbs. No electrical power input would be necessary.

A possibly advantageous method of operation of the motor-pump system is to cycle the helium supply for the pump motor into the laser discharge. For this purpose, the high pressure helium/carbon monoxide supply (see subsection 1.3.2 below) would be equipped with a regulator to supply gas at 240 psi to the motor. After being expanded through the motor, the gas supply would be delivered at 30 psi and 200°K to the discharge injection orifice. In this operating mode, no additional gas storage beyond that necessary for the laser itself would be required.

An alternative method of operation is to separate the pump motor gas supply from that to the laser. The motor supply would be exhausted overboard after use. The advantage of this mode of operation would be that the laser gas supply would be free of trace oil contaminants. However, the supply gas volume would be increased to twice the amount required to operate the laser alone.

It should be noted that operation of the laser using the gases processed by the motor pump will result in a substantial gain increase in the laser optical cavity, since the gases will enter the laser at 200°K rather than 300°K. Accordingly, considerable improvement would perhaps be possible on the performance predictions of the cavity calculations of Section 1.2, which assume 300°K supply gases. In particular, higher powers may be obtainable or, alternatively, operation with a lower Mach number cavity and consequent reduced pumping requirements may be possible. Such total system optimization forms part of the detailed system design study which would be performed after test of various components are completed.

1.3.2 Gas Storage

Premixed helium and carbon monoxide are delivered to the laser from a high pressure storage bottle. Assuming the gas supply is initially pressurized at 2000 psi, the system will operate until the delivery pressure falls below 500 psi. The bottle volume required for ten minutes operation is 1.5 ft^3.

1.4 Summary

A preliminary design study of a compact supersonic flow CO laser has been presented. The basic operating characteristics of the system are:

(i) Power: 20 to 50 watts c.w.

(ii) Wavelengths: 4.7954 to 5.3028 microns, distributed over approximately 15 lines

(iii) Atmospheric absorption coefficient: sea level values vary among lines from .02 km^{-1} to above .1 km^{-1}

(iv) Pumping requirements: 125 cfm

(v) Power supply: 1.5 kw

(vi) Gas supply: He/CO storage 1.5 ft^3 @ 2000 psi for 10 minutes duration.

In the following paragraphs, 2-4, the results of engineering tests on "bread-boarded" versions of key system components for the small scale laser are reported.

2. DISCHARGE OPERATIONAL TESTS

In accordance with the design outlines in Section IV 1.1 above, small discharge tubes equipped with annular slot injector electrodes were built and tested at high gas pressures.

These tests were completed for two discharge tube diameters, 1/2" and 1". Table 9 summarizes performance results for several selected pressures and electrode separations. All runs are for room temperature inlet gases and include an O_2 additive of less than .1% concentration by volume. Note that extremely high power loadings have been achieved, in the range 100-200 kw/lb/sec. Also significant is that CO concentrations of 4.5% can be achieved in the 1/2" diameter tube. It should be noted that gas purity was

TABLE 9

SUMMARY OF SMALL SCALE DISCHARGE OPERATING DATA

Run No.	CO Grade	Discharge Pressure atm	Flow Velocity $cm\text{-}sec^{-1}$	$\dot{m}_{CO}$ $lb\text{-}sec^{-1}$	$\dot{m}_{He}$ $lb\text{-}sec^{-1}$	Discharge Voltage kV	Discharge Current mA	kw/lb/sec (all gases)	% CO	Discharge Tube Diameter inches	Discharge Tube Length inches	kw/lb/sec of CO
1	C.P.	1.0	4.755×10^3	.0006218	.0018743	13.75	23	126.7	4.53	0.5	2.0	508
2	C.P.	1.5	4.947×10^3	.0005100	.0029899	15.7	23	103.2	2.38	0.5	2.0	708
3	C.P.	2.0	5.011×10^3	.0002870	.0041055	16.3	23	85.4	0.99	0.5	2.0	1306
4.	U.H.P.	1.0	1.160×10^3	.0002870	.0018743	12.5	38	210	2.14	1.0	2.0	1655
5	U.H.P.	1.0	1.160×10^3	.0002870	.0018743	17.0	20	157	2.14	1.0	4.0	1184
6	U.H.P.	1.0	1.160×10^3	.0002870	.0018743	12.5	30	173	2.14	1.0	3.0	1306
7	U.H.P.	1.0	1.175×10^3	.0004600	.0018743	14.6	24	150	3.39	1.0	3.0	761
8	C.P.	1.0	1.160×10^3	.0002870	.0018743	13.5	18	112	2.14	1.0	3.0	846
9	U.H.P.	1.0	4.640×10^3	.0002870	.0018743	9.2	40	170	2.14	0.5	2.0	1282
10	U.H.P.	1.0	4.760×10^3	.0006218	.0018743	13.2	25	132	4.53	0.5	2.0	530
11	U.H.P.	1.5	4.947×10^3	.0005100	.0029899	15	25	107	2.38	0.5	2.0	735

found to be important for achieving stable discharge operation at higher CO concentrations. Matheson "Ultra High Purity Grade" CO was used for all runs at CO concentrations above 3%. In addition, a stainless steel trap operating at 400 psi in a dry ice/methanol bath removes condensable impurities from the carbon monoxide supply. A copper coil following the trap returns the CO to laboratory temperature.

3. NOZZLE OPERATIONAL TESTS

A small wedge nozzle was constructed in accordance with the design outlined in Section IV 1.2 above, and gas dynamic tests were performed. Nozzle dimensions are shown in Figure 13; construction was entirely of plexiglass. Static pressures were measured at eight taps along the nozzle centerline at several expansion area ratios.

The nozzle was mounted on a 1-foot section of 4-inch I.D. copper pipe which was pumped by the Calspan vacuum sphere through a 2-inch I.D. copper line. Static pressure measurements down the nozzle revealed that a Mach number of 4 was achieved at an expansion area ratio of 8. However, at higher expansion ratios the static pressure rose, presumably due to boundary layer separation and a resulting shock phenomenon. It is probable that this gas dynamic limitation can be circumvented in a practical system by using a properly designed supersonic diffuser. For the purposes of laboratory testing, however, the nozzle was merely remounted directly on a 16 in. dia. vacuum line; this resulted in an immediate gas dynamic performance improvement.

Figures 14-16 summarize the nozzle performance in this configuration for three discharge pressures: 1, 1.5, and 2 atmospheres. In these figures, nozzle static pressure is plotted against the expansion area ratio in the nozzle, i.e., the ratio of the nozzle cross sectional area to the nozzle throat cross sectional area. Comparison is made with the predictions of an ideal isentropic expansion calculation (solid curve). In all three cases plotted, the CO percentage concentration was chosen to be commensurate with stable discharge operation at the selected pressure, as determined from the discharge tests reported in Section IV, 2 above. It can be observed that an actual performance

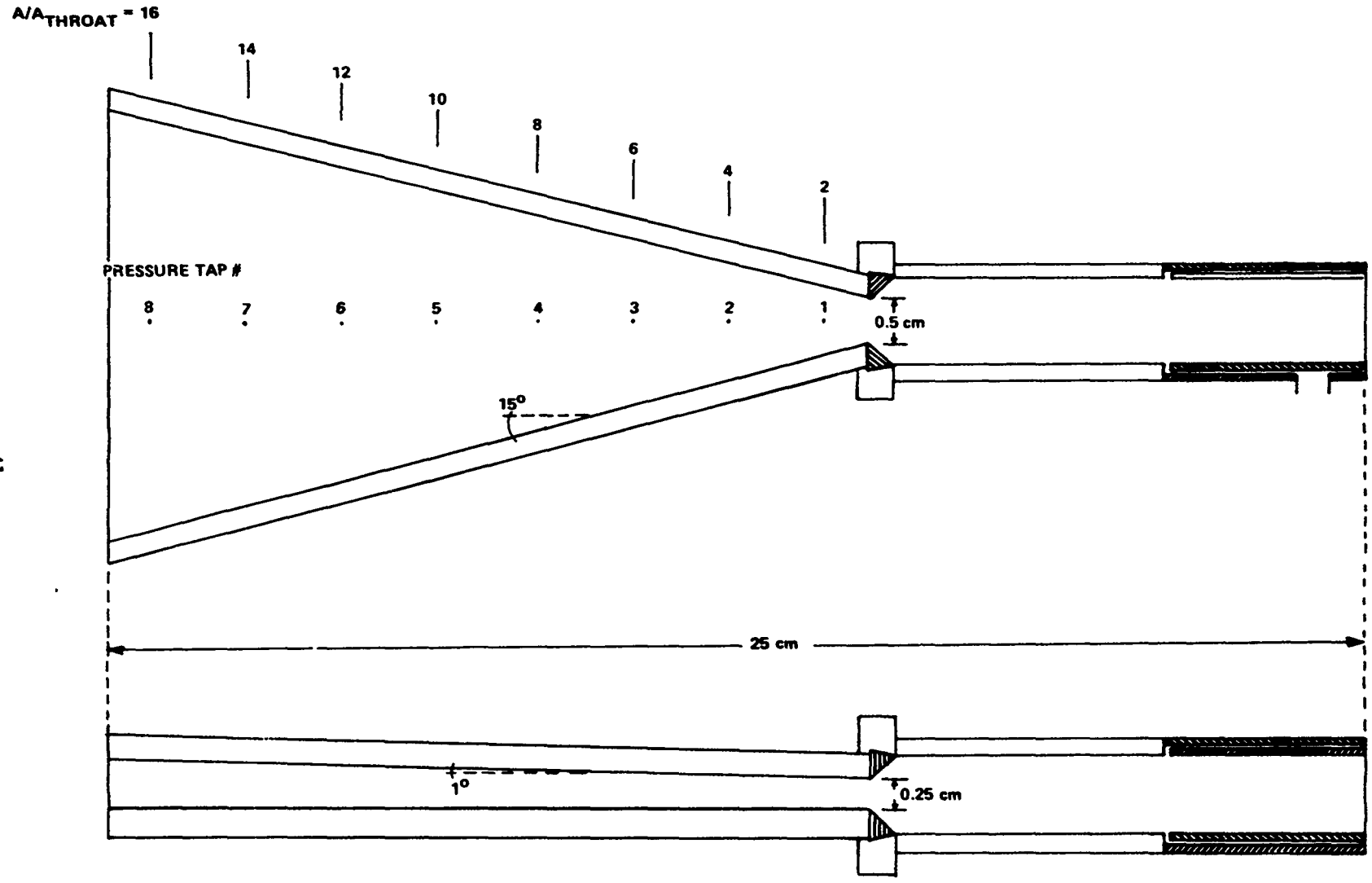

Figure 13 SCHEMATIC OF SMALL SCALE LASER DISCHARGE AND NOZZLE ASSEMBLY

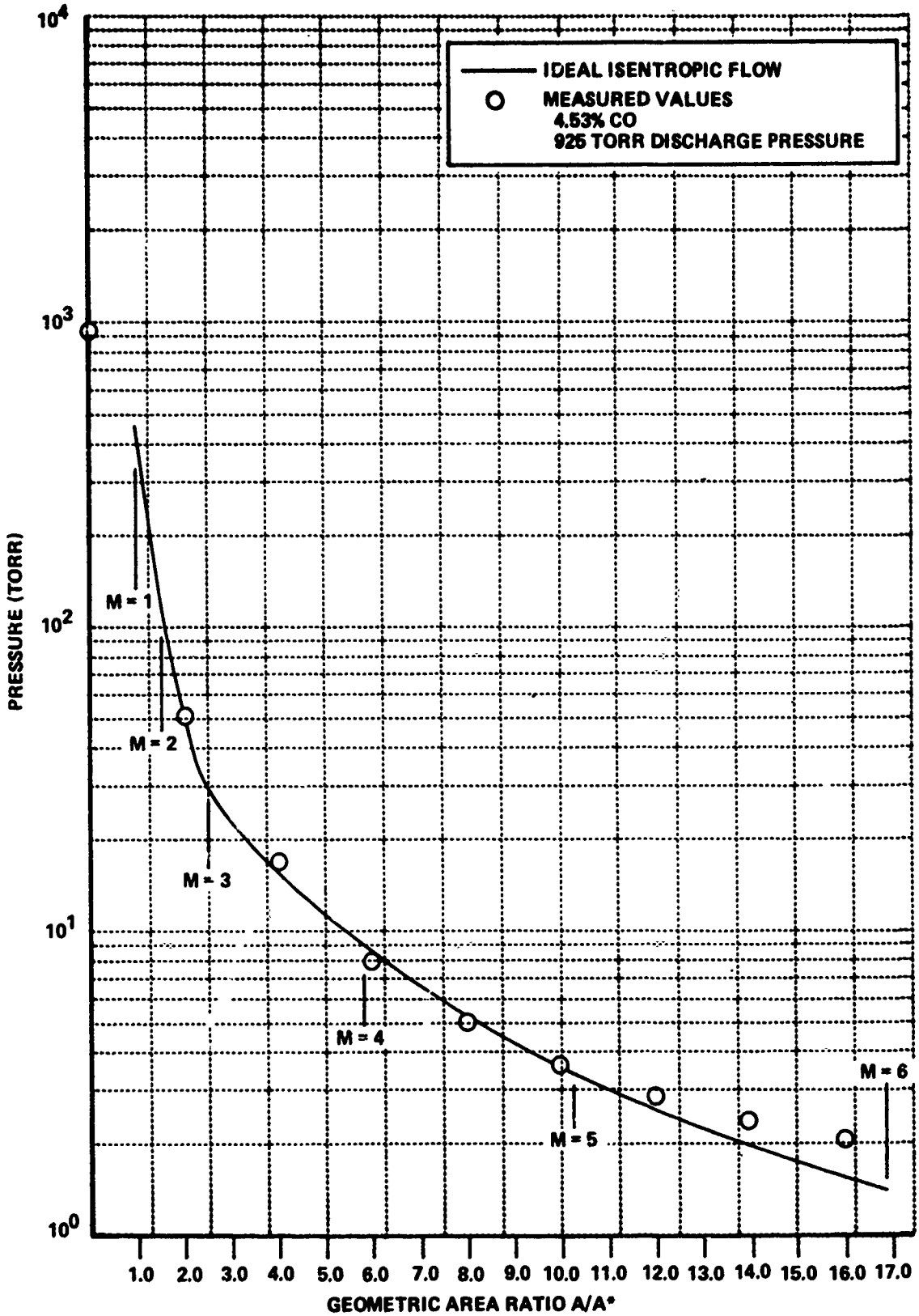

Figure 14 PRESSURE DISTRIBUTION THROUGH SMALL SCALE NOZZLE, 1.0 ATMOSPHERE OPERATING PRESSURE

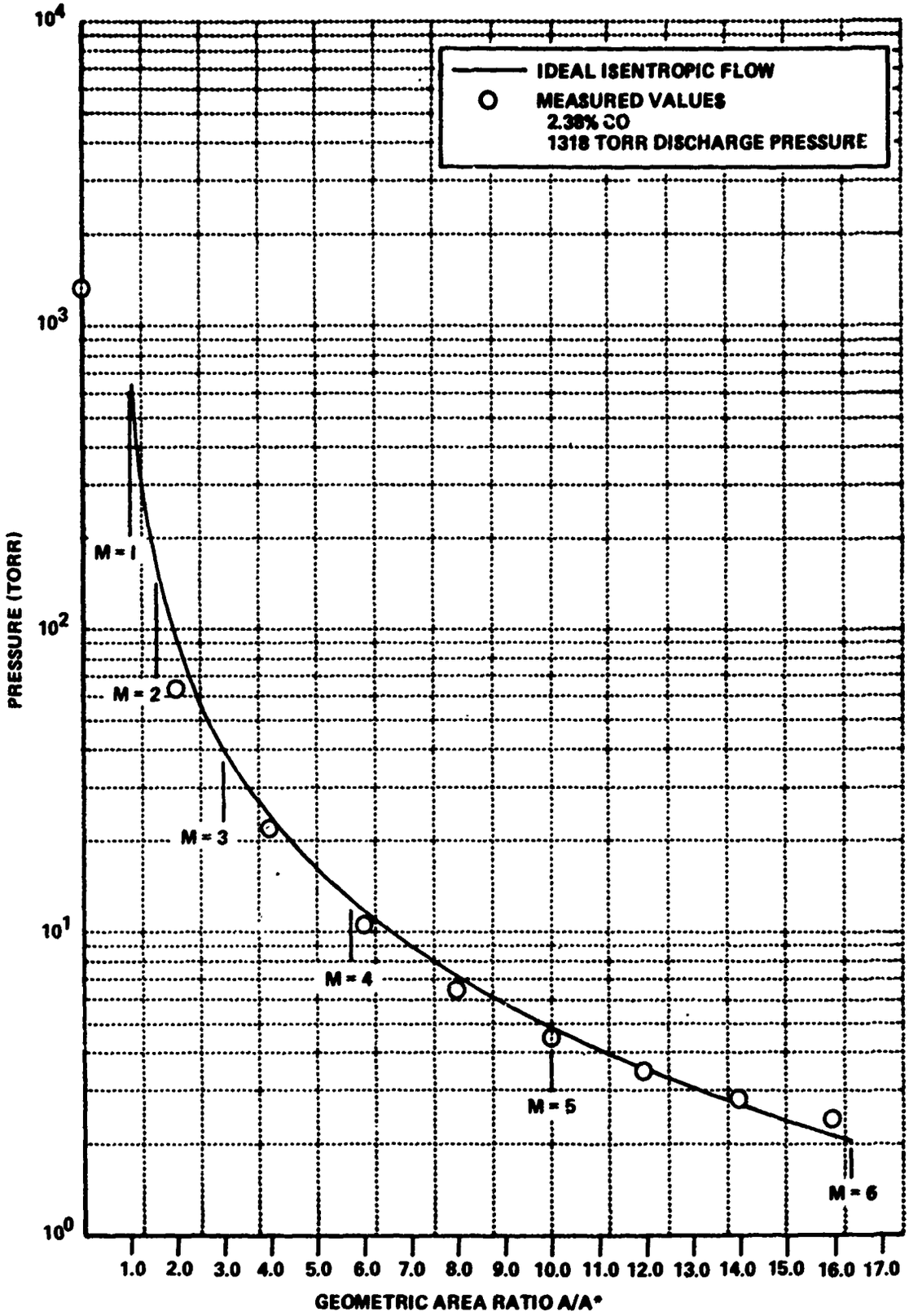

Figure 15 PRESSURE DISTRIBUTION THROUGH SMALL SCALE NOZZLE, 1.5 ATMOSPHERE OPERATING PRESSURE

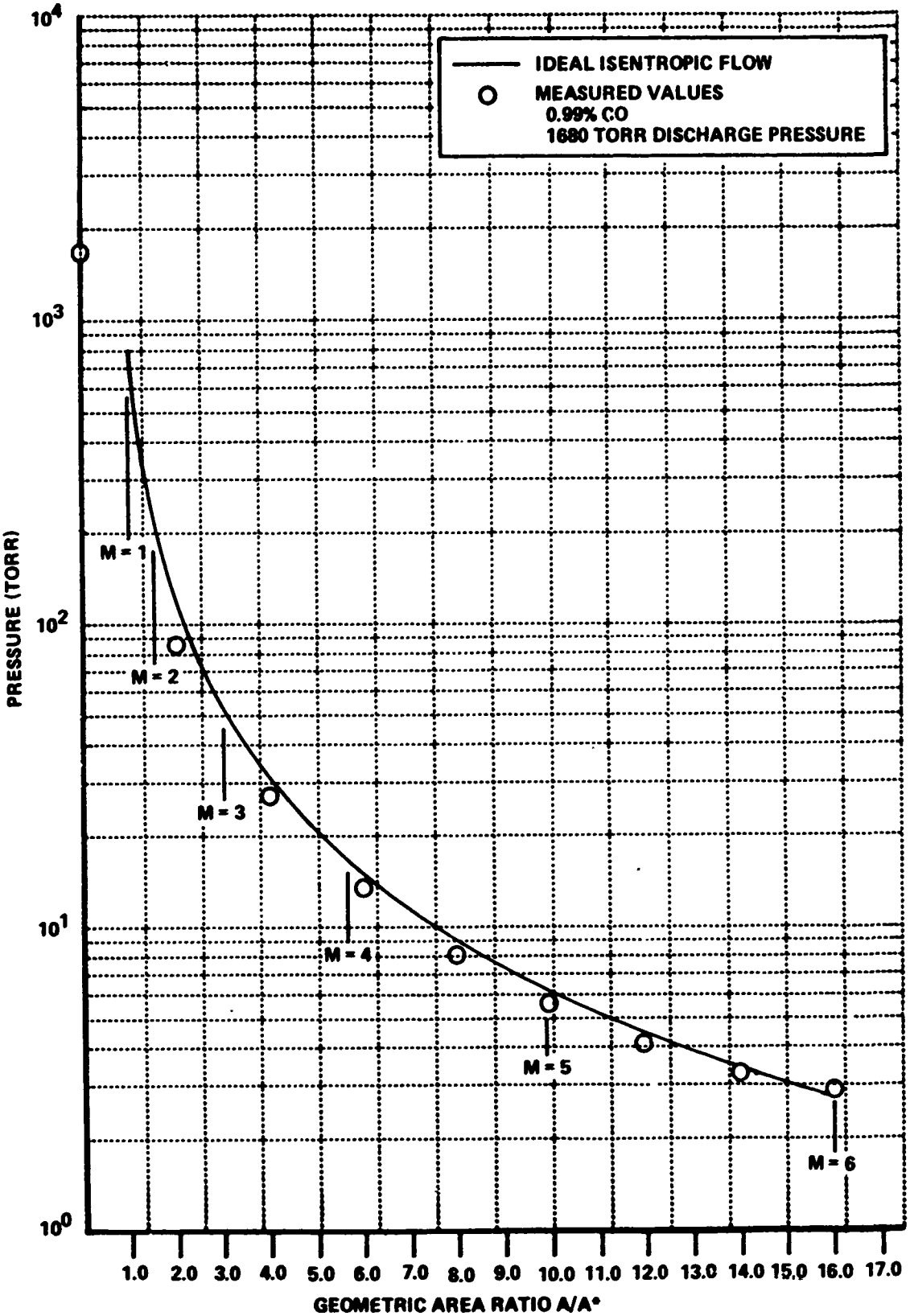

Figure 16 PRESSURE DISTRIBUTION THROUGH SMALL SCALE NOZZLE,2.0 ATMOSPHERE OPERATING PRESSURE

is very close to the ideal prediction from the throat to expansion ratio $A/A^* = 16$. Expansion to this area ratio corresponds to an in-cavity Mach number of 6, and a ratio of cavity to discharge gas temperature of $T_{\text{Optical Cavity}}/T_{\text{Discharge}} = .08$. Thus, if the temperature of gases leaving the discharge is 375°K, the in-cavity gas temperature would be 30°K, at $A/A^* = 16$.

These results further indicate that extremely high performance of these small nozzles will be practical when using a carefully designed supersonic diffuser.

4. LASER OPERATIONAL TESTS

In view of the excellent gas dynamic performance of the small scale nozzle and satisfactory power loading of the small scale discharge, internal mirrors were placed on the system to investigate preliminary lasing characteristics of a laser of these dimensions. The discharge section, as fully described in Section IV, 1.1 above, consisted of a 1/2" diameter tube at an electrode separation of 2". The resonantor cavity was formed by a 1" diameter, 4 meter radius of curvature total reflector and a 1" diameter 95% reflecting germanium flat. The following subsections present the results obtained with the laser cavity at nozzle area ratios 8 and 16.

4.1 Operation at Area Ratio 8

Cavity location at $A/A^* = 8$ gives an active medium cavity length of only 1-5/8". The gas flow at this point is at a supersonic Mach number of 4.5, and the in-cavity gas temperature, assuming a 375°K discharge exit temperature, is estimated to be $\sim$ 50°K. With cavity output coupling of 5%, discharge pressure at 1 atmosphere, and a 4.5% CO gas mixture, 1.5 watts power output was obtained. However, detailed optimization of the cavity design needs to be carried out. This is evidenced by the fact that at the above operating conditions, 5 watts power output was obtained when the streamwise cavity length was increased from .250" to .375". At the 5 watt level mass efficiency was 2 kw/lb/sec and electrical efficiency 2%. It is evident that attention must be directed to various possible

optical configurations, including extending the streamwise cavity length, multi-passing the cavity by mirror folding, etc.

4.2 Operation at Area Ratio 16

Cavity location at A/A* = 16 gives an active medium cavity length of 3-1/4". The gas flow at this point is at a supersonic Mach number of 6, and the in-cavity gas temperature is estimated to be ~ 35°K. Figures 17 and 18 summarize laser performance for the cavity of this location.

Figure 17 shows operation at the 1 atmosphere discharge pressure level. The output spectrum of the laser is shown. The height of each spectral line is proportional to the fraction of the total laser power in the line. The horizontal scale is wavelength in microns. For Figure 17, 71% of the total laser power is below 5.0 μ, and 88% is below 5.1 μ. Figure 18 is a similar plot, but for operation at the 1.5 atmosphere discharge pressure level. For this case, 68% of the total laser power is below 5.0 μ, and 89% is below 5.1 μ. The other operating parameters of the laser are indicated on the plots.

The spectral shift to shorter wavelengths shown in these data is quite marked. The spectral distribution from a conventional liquid nitrogen wall-bath-cooled CO laser is shown on the plots for comparison.

Tables 10 and 11 list the line identifications and wave-length assignments for the data plotted in Figures 17 and 18.

Figure 19 is a plot of experimental data for laser output versus cavity output coupling. It is seen that an output coupling near 5% is optimum for this laser system.

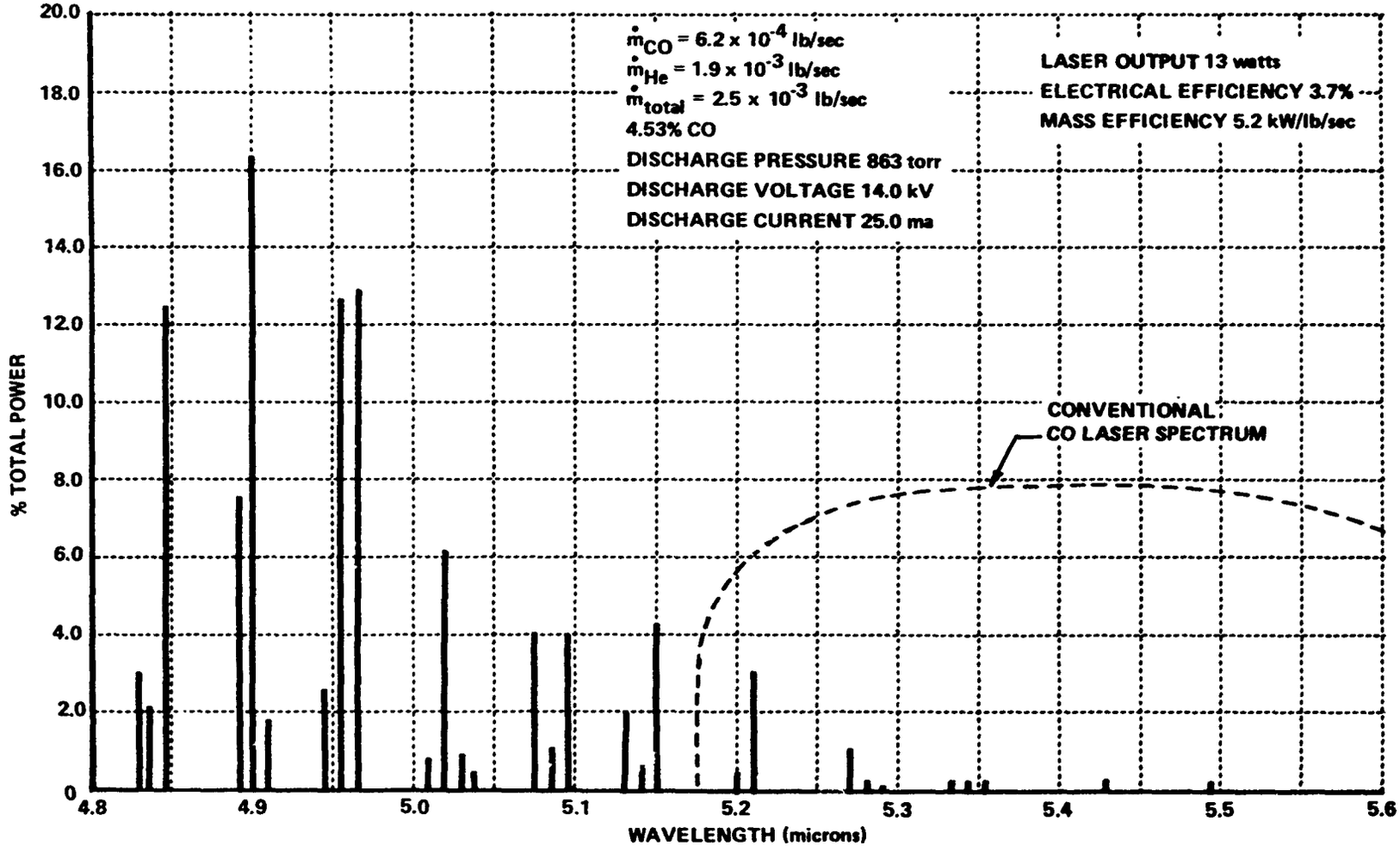

Figure 17 *SMALL SCALE LASER OPERATION, 1.0 ATMOSPHERE DISCHARGE PRESSURE*

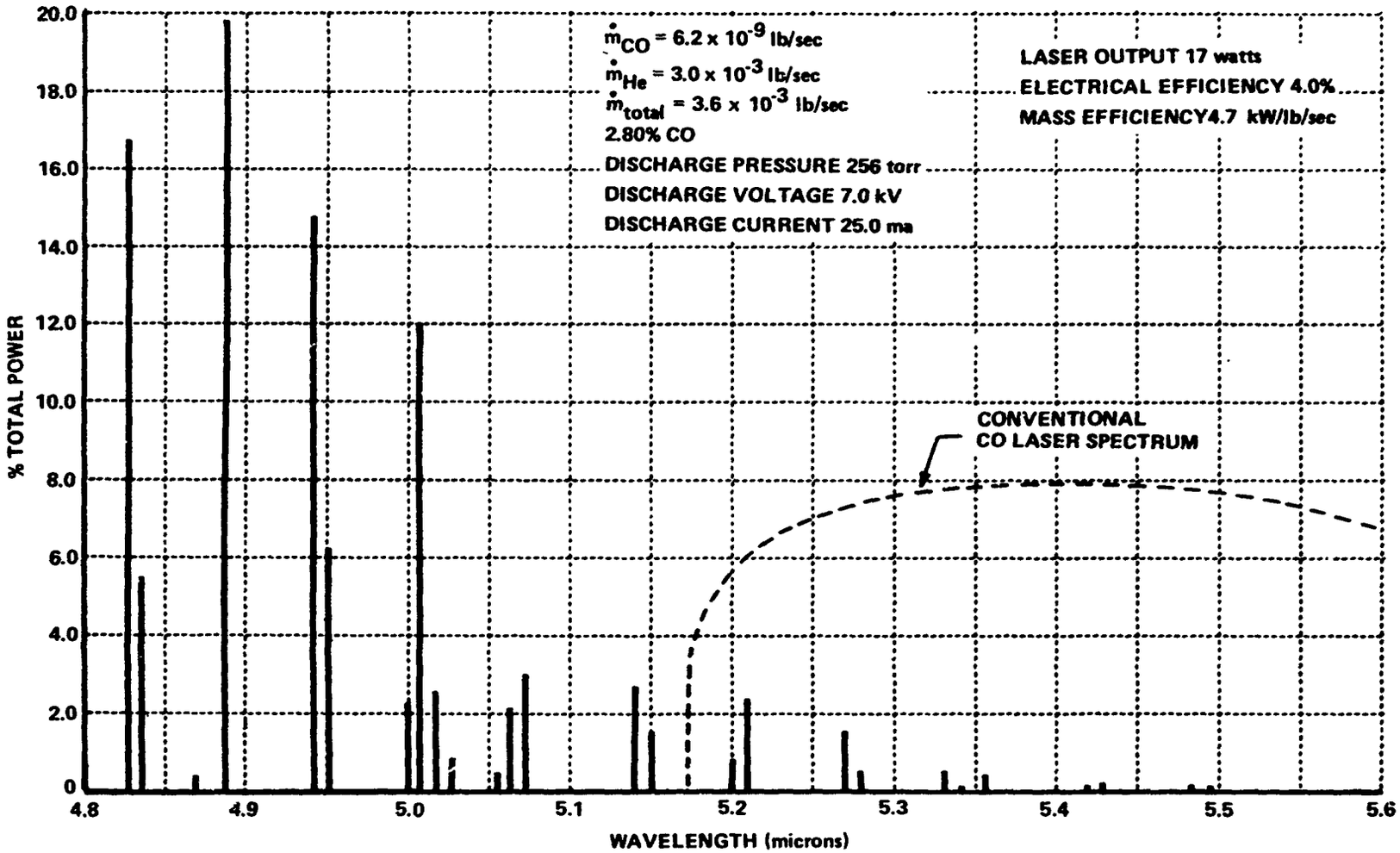

Figure 18 SMALL SCALE LASER OPERATION, 1.5 ATMOSPHERE DISCHARGE PRESSURE

TABLE 10

SMALL SCALE LASER EXPERIMENTAL OUTPUT SPECTRA

M = 6, P_0 = 1 atmosphere

Vibrational Band	Rotational Line	λ μ	% of Total Output
3-2	P(5)	4.82821	3.006
	P(6)	4.83743	2.129
	P(7)	4.84677	12.398
4-3	P(5)	4.89001	7.514
	P(6)	4.89936	16.155
	P(7)	4.90885	1.828
5-4	P(4)	4.94383	2.505
	P(5)	4.95318	12.586
	P(6)	4.96271	12.836
6-5	P(4)	5.00825	.726
	P(5)	5.01783	6.136
	P(6)	5.02752	.839
	P(7)	5.03734	.363
7-6	P(4)	5.07441	3.970
	P(5)	5.08398	.977
	P(6)	5.09385	3.719
8-7	P(3)	5.13228	2.041
	P(4)	5.14205	.589
	P(5)	5.15169	4.170
9-8	P(3)	5.20135	.394
	P(4)	5.21129	2.971
10-9	P(3)	5.27209	1.093
	P(4)	5.28222	.183
	P(5)	5.29196	.013
11-10	P(2)	5.33443	.294
	P(3)	5.34459	.115
	P(4)	5.35489	.239
12-11	P(4)	5.42933	.180
13-12	P(3)	5.49496	.031

TABLE II

SMALL SCALE LASER EXPERIMENTAL OUTPUT SPECTRA

$M = 6$, $P_0 = 1.5$ atmosphere

Vibrational Band	Rotational Line	λ μ	% of Total Output
3-2	P(5)	4.82821	16.671
	P(6)	4.83743	5.466
4-3	P(3)	4.87159	.410
	P(5)	4.89001	19.759
	P(6)	4.89936	2.569
5-4	P(4)	4.94383	14.785
	P(5)	4.95318	6.176
6-5	P(3)	4.99880	2.186
	P(4)	5.00825	11.984
	P(5)	5.01783	2.473
	P(6)	5.02752	.820
7-6	P(2)	5.05516	.410
	P(3)	5.06465	2.145
	P(4)	5.07441	3.047
8-7	P(3)	5.13228	.924
	P(4)	5.14205	2.580
	P(5)	5.15169	1.514
9-8	P(3)	5.20099	.818
	P(4)	5.21129	2.338
10-9	P(2)	5.26180	.034
	P(3)	5.27209	1.503
	P(4)	5.28222	.186
11-10	P(2)	5.33443	.458
	P(3)	5.34459	.031
	P(4)	5.35489	.361
12-11	P(3)	5.41791	.096
	P(4)	5.42933	.155
13-12	P(2)	5.48320	.014
	P(3)	5.49496	.088

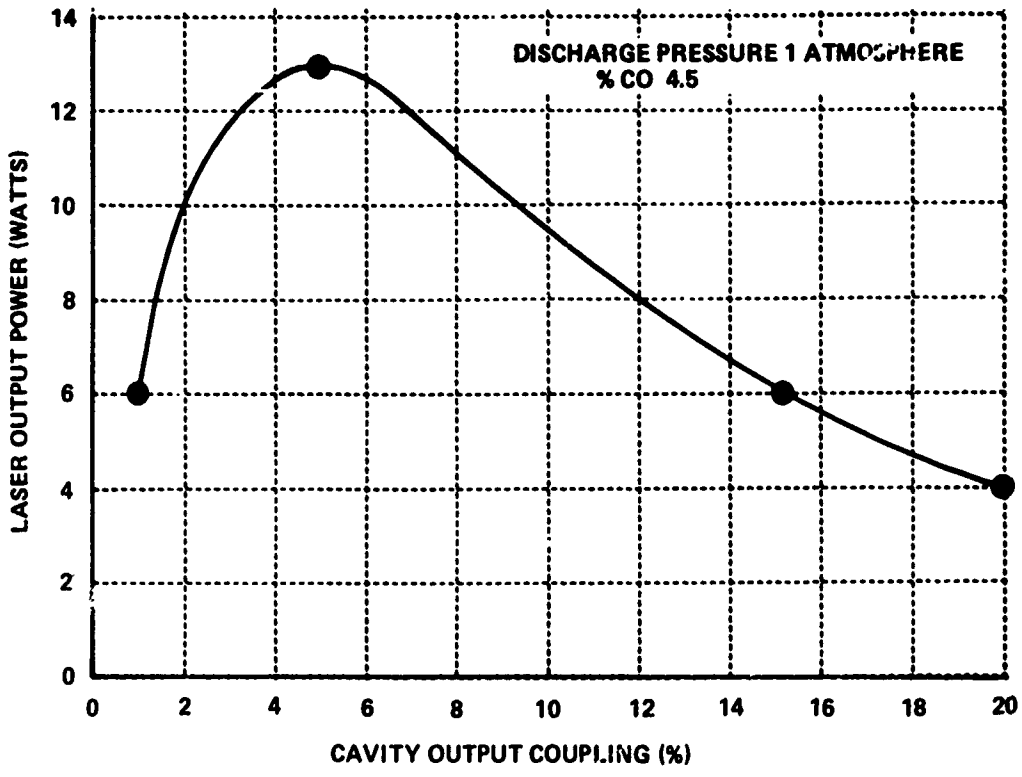

Figure 19 SMALL SCALE LASER, POWER VS. OUTPUT COUPLING

Section V
SUMMARY AND CONCLUSIONS

1. PRESENT PERFORMANCE LEVELS

During the past year, work has concentrated on the development of an aerodynamically stabilized glow discharge technique and on research and development of two supersonic flow lasers, one operating at 11 gm/sec mass flows and the other a much smaller, 1.5 gm/sec device. Both these lasers, using the aerodynamically stabilized glow discharge technique, have operated at discharge plenum pressures in excess of 1 atmosphere. The following performance levels have been achieved:

(1) The 11 gm/sec device, operating at atmospheric discharge pressure, produces 350 watts cw at 11% efficiency, with greater than 60% of its power in the 4.8 to 5.1 micron range.

(2) The 1.5 gm/sec device, operating at discharge pressures in excess of 1.5 atmospheres, produce 17 watts cw at 4% electrical efficiency, with 90% of its power in the 4.8 to 5.1 micron range.

Table 12 summarizes the gas dynamic performances of the 1.5 gm/sec device at the two expansion ratios for which lasing data have been obtained. It will be noted that volumetric flow rate requirements are within the range predicted in the preliminary analytical study of the small scale laser, as given in Table 7 of this report. The actual operating data of the prototype small scale device, as given in Table 12, are the most encouraging results of the past year's program. As discussed in Section IV, it is anticipated that optimization of the optical cavity design should substantially increase the powers obtained to date.

2. DEVELOPMENT POTENTIAL

Three areas can be identified in which further development should substantially improve the performance of this class of gas lasers. These are:

TABLE 12

SMALL SCALE LASER, SUMMARY OF EXPERIMENTAL OPERATING DATA

Expansion Area Ratio A/A_{Throat}	Cavity Length cm	Cavity Mach Number	Cavity Temperature °K	Laser Power Out, Watts	Efficiency %	Volumetric Flow Rate After Normal Shock Recovery, cfm
8	4	4.6	52	5	2	112 @ 111 torr, 390°K
16	8	6.0	33	17	4	223 @ 56 torr, 402°K

(i) Additional optimization of the high pressure discharge design. In particular, varying the operating parameters of the gas injector system (slot width, injector pressure) may enable substantial increases in discharge operating pressure above the 1.5 atmosphere level already obtained.

(ii) Supersonic diffuser design and development. The normal shock recovery volumetric flow rates indicated in Table 12 offer the promise of relatively small pumping requirements for the 1.5 gm/sec laser, if a high performance supersonic diffuser can be designed for use with this system.

(iii) Optical cavity optimization. As shown in Section IV, computer modeling calculations indicate a much larger amount of available power in the CO vibrational mode of the 1.5 gm/sec laser than is actually extracted in the experimental device (Table 12). The relatively low power extraction is a consequence of the short gain path of the cavity combined with the short streamwise length of the cavity. A careful design of an optimized cavity based on additional analytical studies should substantially improve performance.

3. SUMMARY

Electrically excited carbon monoxide lasers have been developed which produce the bulk of their power in the 4.8 to 5.1 micron wavelength range. The lasers utilize an aerodynamically stablized, i.e., glow discharges, which have been successfully operated to pressures of 1.5 atmospheres in CO-He laser gas mixtures. Small versions of these lasers, producing c.w. power in the 20 watt range, can be operated with pumping systems of approximately 100 cfm capacity.

APPENDIX

AIAA Paper presented at 12th Aerospace Sciences Meeting. To be published AIAA Journal, Jan. 1975.

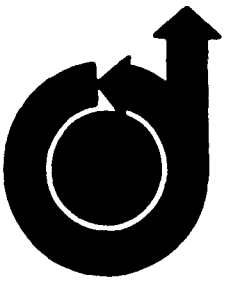

AIAA Paper No. 74-179

EXPERIMENTAL AND THEORETICAL INVESTIGATION OF THE ELECTRICALLY EXCITED, SUPERSONIC FLOW CARBON MONOXIDE LASER

by
J. W. RICH, R. C. BERGMAN,
and
J. A. LORDI
CALSPAN Corporation
Buffalo, New York

AIAA 12th Aerospace Sciences Meeting

WASHINGTON, D.C. / JANUARY 30-FEBRUARY 1, 1974

EXPERIMENTAL AND THEORETICAL INVESTIGATION OF THE ELECTRICALLY EXCITED, SUPERSONIC FLOW CARBON MONOXIDE LASER*

J. W. Rich[+], R. C. Bergman[++], and J. A. Lordi[+++]
Calspan Corporation, Buffalo, N. Y. 14221

ABSTRACT

A study of CW electric-discharge-excited supersonic flow carbon monoxide lasers is presented. Recent experimental results are reported for a device utilizing a high pressure glow discharge in the plenum of a supersonic nozzle. An optical cavity is established transverse to the supersonic flow at an effective nozzle area ratio of $A/A^* = 8.9$. CW powers in excess of 300 watts and efficiencies of 10% are obtained. More than 60% of the output power is at wavelengths below 5.10 microns. The experimental data are compared with the predictions of a computer model of the laser performance.

*This research was supported by the United States Air Force Avionics Laboratory under Contract F33615-73-C-1285 and United States Army Missile Command and Advanced Research Projects Agency, Contract DAAH01-72-C-0936 under ARPA Order No. 1180.

[+]Principal Engineer, Aerodynamic Research Department
[++]Assistant Physicist, Aerodynamic Research Department
[+++]Principal Engineer, Aerodynamic Research Department, Member AIAA

1. INTRODUCTION

The direct-discharge-excited carbon monoxide laser has demonstrated the remarkable efficiency of a glow discharge for exciting the vibrational quantum states of CO.[1-3] Continuous wave operation of carbon monoxide lasers has been achieved in which nearly 50% of the input electrical power is converted into laser output on the fundamental vibration-rotation bands.[4] This efficiency is the highest reported for any cw laser, and makes the CO laser an attractive candidate for many IR applications. There are, however, some significant problems associated with the use of powerful CO lasers. Of direct concern to the present work is that the output wavelengths of conventional CO lasers operating at peak efficiency are from 5.1 microns to 5.6 microns. This output corresponds to vibrational bands $V = 6 \rightarrow 5$ to $V = 17 \rightarrow 16$. Unfortunately, part of the ν_2 bands of water vapor also occur in this wavelength range. Many of the most powerful CO laser spectral lines are significantly attenuated during transmission through the atmosphere, due to absorption by the wing of R-branch $\nu_c \rightarrow \nu_2$ transitions in H_2O. A second problem is that the techniques used to maximize efficiency are costly, and are not necessarily scalable to large devices. Specifically, conventional CO lasers use discharge tubes cooled by static wall baths. Peak efficiency is reported with liquid N_2 cooling; efficiency is reduced by 90% under room temperature operating conditions. Secondly, at both room temperature and cryogenic temperature conditions, xenon is used as a gas additive; operation without Xe also greatly reduces efficiency.

The present paper discusses the performance of an electrically excited carbon monoxide laser which utilizes gas dynamic cooling. This laser was designed to eliminate the problems discussed in the preceding paragraph. A preliminary report of the laser was published at an early stage of development.[5]

The use of gas dynamic cooling in a CO laser was motivated by theoretical studies[6-10] of vibrational energy exchange processes in CO laser gas environments. These studies suggested that high output power from vibrational bands below $V = 6 \rightarrow 5$ could be obtained, if the gas translational temperature were lower than that obtainable in statically cooled discharge tubes. Laser output on bands below $V = 6 \rightarrow 5$ in CO corresponds to wavelengths below

5.1 microns; such wavelengths can be more suitable for atmospheric transmission, as they are less overlapped by water vapor absorption bands. This prediction of shorter wavelength output with decreasing temperature has been verified by experiments in shock tunnels.[11-12] In these experiments, high-temperature mixtures of CO and Ar, created behind a reflected shock in a shock tube, were expanded in a supersonic nozzle. Optical cavities, established transverse to the flow at large expansion area ratios ($A/A_{throat} > 500$), create powerful cw laser action for the duration of the steady flow. McKenzie[11] has shown that more than 50% of the output from such a system can be from wavelengths below 5.0 μ, i.e., from vibrational levels V = 5 and below. It should be noted, however, that thermal excitation of the laser gases is a relatively inefficient means of energizing the vibrational mode of CO. At the 2000°K plenum conditions of the shock-tunnel-driven CO gas-dynamic lasers, only $\sim$ 20% of the equilibrium thermal energy is in the vibrational mode. This percentage represents an inherent upper limit on the maximum efficiency of a thermally excited CO gas-dynamic laser. Such a system cannot, therefore, attain the efficiencies already achieved in discharge-excited CO lasers. For this reason, the laser discussed in the present paper uses an electric discharge to energize the CO vibrational mode.

The following sections report the results of experimental and analytical studies in the electrically excited supersonic flow CO laser. Section 2 describes the laser, and presents results of performance and diagnostic experiments in the device. Section 3 summarizes theoretical models and numerical codes used to analyze the laser performance, and gives a comparison with experimental results. A summary and some conclusions are given in Section 4.

2. EXPERIMENTAL STUDIES

2.1 Laser Geometry

Figure 1 shows a perspective schematic sketch of the electrically excited gas dynamic carbon monoxide laser. Fig. 2 gives the critical dimensions of the laser. Photographs of the actual device are given in Figures 3 and 4. The laser uses a direct current electrical discharge to excite a mixture

of CO and He; subsequent to excitation, the gas mixture is cooled by a supersonic gas dynamic expansion. Referring to Figures 1 and 2, the discharge tube consists of a 1-1/2 inch i.d. pyrex pipe, which forms the plenum chamber of the supersonic nozzle. The anode is a water-cooled hollow brass and copper pipe which also functions as a gas-dynamically choked orifice through which the premixed gases are injected into the discharge tube. Details of the anode design are discussed in the following section. The cathode is formed by the nozzle throat itself, which is a water-cooled brass section, with throat dimensions of 1.2 x 1.1 cm. The nozzle is of rectangular cross section, as shown. The expansion half-angle is 15°, and the top and bottom surfaces diverge slightly to allow for boundary-layer growth. The system currently is being pumped by the Calspan flow laser facility, which consists of a 125,000 ft^3 vacuum sphere backed by 850 cfm vacuum pumps. Use of this facility to pump the laser permits essentially continuous supersonic operation.

2.2 Discharge Operating Characteristics

The laser has been operated at discharge pressures from less than 0.5 atmospheres to 1.5 atmospheres. Operating pressures in this range are obtainable only with a large preponderance of helium diluent. Reduction of the amount of helium diluent creates discharge instabilities which very rapidly result in arc breakdown of the discharge. The use of diluents other than helium gave unsatisfactory results; the maximum discharge pressures obtainable were quite low, and laser performance was in no way comparable to those achieved with helium. The role of helium in increasing discharge stability is, apparently, to insure rapid dissipation of local arc filament "hot spots" by increasing the heat conductivity of the discharge gases. Such heat dissipation prevents growth of arc filaments and subsequent arc breakdown of the discharge. It should be noted that, unlike CO_2 gas dynamic lasers, helium plays no critical role in enhancing pumping of the population inversion. Indeed, helium, as a fast vibration-to-translation (V-T) relaxer, potentially can degrade the population inversions in a CO laser. Secondly, unlike conventional wall-cooled CO lasers, helium is not required to insure rapid thermal transport to cold walls. The validity of these two points is demonstrated by the operation of the thermally excited CO gas dynamic lasers previously mentioned. [11-12]

These systems, not using an electric discharge, do not require the stabilizing effect of helium, and perform quite well with either argon or nitrogen diluents.

Most of the data presented in this paper were obtained at a discharge pressure of 350 torr. At this pressure, the upstream electrode (the anode) consisted of a 1/2" i.d. pipe, through which gases were injected at sonic velocity parallel to the discharge axis. Recently, however, stable discharge operation has been achieved at supra-atmospheric pressures (to 1.5 atmospheres) using an annular slot injector anode similar to that developed by Gibbs and McLeary.[13] In this configuration, the anode is in the form of a 1" i.d. pipe, which contained a circumferential slot through which gases were injected normally to the discharge axis. The slot width is just sufficient to choke the gas flow. This method of gas injection creates a radial flow velocity component in the vicinity of the anode. As discussed in detail in Ref. 13, this velocity component promotes the rapid dissipation of incipient streamwise arc filaments, and thereby increases discharge stability.

The power supplies used for the laser are Universal Voltronics D.C. voltage regulated supplies, equipped with saturable core reactor current limiting circuits. With the current limiter, it is possible to prevent large current surges which precede total arc breakdown of the discharge. Operation with the current limiter significantly extends the stable operating region of the discharge, permitting operation at currents into the arc transition region. It should be noted that series ballast resistance is minimal in the present setup, amounting to less than 1% of the discharge impedance. The discharge has a positive voltage-current characteristic. During normal operation, the milky-blue glow of the positive column of the CO/He discharge fills the discharge tube with a fairly uniform intensity. A photograph of this glow is in Fig. 4.

2.2 Gas Dynamic Performance

The principal gas dynamic diagnostic in the laser is the measurement of wall static pressure. There are pressure measurement taps at each station indicated in Fig. 2. These taps are located in the bottom wall of the nozzle close to the centerline. Pressures are measured with an MKS Industries

"Baratron" gauge. Static pressure in the discharge section can also be measured at both the upstream and downstream ends of the discharge tube, as indicated in Fig. 2. Under the present operating conditions of the laser, the upstream and downstream discharge pressure measurements are essentially equal; the flow velocity in the discharge tube is sufficiently slow that the discharge static pressure measurement can be taken as equal to the stagnation pressure.

Figure 5 shows the static pressure distribution down the nozzle for the typical operating conditions indicated on the graph. Also shown are the Mach number variation, as calculated from the pressure measurements, and a comparison with the pressure and Mach number distribution predicted for an ideal isentropic nozzle. From these data, it can be seen that the laser shows considerable departure from the isentopic nozzle prediction at higher expansion ratios. This departure can be attributed to two causes: 1) boundary layer growth, which is particularly marked at the low density, high expansion portion of the nozzle, and 2) the highly nonequilibrium kinetic processes occurring in the gas flow, specifically, the influence of nonequilibrium vibrational processes.

The supersonic flow pattern as given in Fig. 5 will remain steady as long as the pressure at the nozzle exit does not become too large. However, when the pressure in the vacuum sphere rises to several times the nozzle static pressure at the farthest downstream station (#1), a shock pattern moves up the nozzle, destroying the supersonic flow. This phenomenon is shown in Fig. 6, in which static pressure and laser power at nozzle Station No. 1 are plotted as functions of time.* These data show that supersonic flow is definitely required to sustain lasing operating in the present configuration. It can be noted from Fig. 6 that, after flow initiation at $t = 0$, the static pressure in the cavity quickly rises to a steady "plateau" of approximately 1.5 torr. After discharge initiation (at $t \approx 4$ sec), laser power also is established at a steady value of approximately 15 watts. At approximately 65 seconds, static pressure

*The data of Fig. 6 were deliberately selected to illustrate a limited-pumping-capacity case, in which back pressure quickly rose to a value sufficient to create separation. The run times and the laser power given in Fig. 6 are not typical of the current performance levels of the system.

in the cavity begins to rise. This rise in static pressure is due to a flow separation phenomenon. Back pressure at the nozzle exit has risen to a value such that the flow is separating from the regions near the nozzle walls, and a separation shock system begins to move through the laser cavity. It can be observed that laser power now begins to fall off. Pressure continues to rise until all supersonic flow ends at approximately t = 135 sec, and laser output ceases entirely.

2.3 Optics

The optical cavity in the laser was established using a mirror system consisting of a 4 meter radius of curvature total reflector and a dielectric-coated germanium flat. The mirrors were obtained commercially. The mirrors are internally mounted, in cylindrical mirror boxes which can be bolted in place at any of the nozzle stations shown in Fig. 2. The laser data reported in this paper were all obtained with an optical cavity at the farthest downstream location in the nozzle, Station No. 1 in Fig. 2.

2.4 Laser Performance

Figures 7 and 8 illustrate the laser performance at the 350 torr discharge level. These data were obtained with the straight axial flow injector anode. Figure 7 is a plot of the laser power versus the CO flow rate. Results are shown for various discharge currents in the range 20 to 90 ma. It can be seen that laser power increases monatonically with CO flow rate for all values of the discharge current. Above 80-90 ma, the discharge arced, and data were unobtainable. It should also be noted that at the higher CO flow rates, power reaches a maximum at currents of approximately 70-80 ma; operation at currents above this range did not increase output power. Finally, at CO flow rates above the maximum shown (4.2×10^{-3} lbs/sec), the discharge became quite unstable; continuous glow discharge operation was not possible. At the maximum CO flow rate of 4.2×10^{-3} lbs/sec, CO comprised 5% by volume of the gas in the discharge; the remainder of the mixture was helium. If the fraction of CO in the mixture is raised much above 5%, the thermal conductivity of the gas mixture becomes significantly reduced. It is this reduction of thermal conductivity that probably causes the onset of arc instabilities

with increasing CO concentration. At high CO concentrations, heat dissipation from incipient arc filaments is reduced; increasing temperature in these filaments causes a reduction in the local gas number density. The increased local E/N ratio causes increased ionization in the filament, resulting in increased local current and filament growth, and leads to arc breakdown.

Operation of the discharge at currents above approximately 65 ma caused a decrease in efficiency, although laser power increased in some cases. This is illustrated in Fig. 8, in which efficiency is plotted against discharge current, for several values of the CO flow rate. Efficiency is defined as the per cent of electrical input power recovered as laser output radiation. Figure 8 also shows a continuous increase in efficiency with CO flow rate, for almost all values of discharge current.

Figures 9 and 10 illustrate the laser performance at higher discharge pressures, which were achieved using the annular slot injector anode of Ref. 13. Figure 9 plots laser power and efficiency versus discharge current, for a discharge pressure of 685 torr. The gases are entering the discharge at room temperature. The gas mass-flow rates and volumetric concentrations are indicated on the figure. Maximum power achieved was 360 watts at 11% efficiency. Figure 10 shows results of a preliminary effort to assess the effect of increased CO concentration. In order to strike the discharge at higher CO concentrations, it was necessary to operate at the lower total pressure of 495 torr. The discharge was stable with CO concentration up to 15% and power increased with CO concentration.

Finally, Table 1 presents some preliminary results of operation of the laser at supra-atmospheric discharge pressures. Three cases are shown, all for discharge pressures of 1.5 atmospheres. Stable discharge operation was obtained, but the percentage of CO was relatively small, being less than 4%. Accordingly, the mass efficiency (kw/lb/sec) is lower than for operation below 1 atmosphere.

In Run nos. 1 and 2 of Table 1, room temperature inlet gases were used. CO concentration was increased from 1.99% in Run 1 to 3.26% in Run 2, reaching a maximum mass efficiency of 9.17 kw/lb/sec and an electrical efficiency of 10.4%. In Run no. 3, gases precooled to 200°K were used, with a consequent increase in electrical efficiency to 11%. However, mass efficiency is somewhat less than the highest achieved with room temperature operation. It should be noted that pressures above 1.5 atmospheres are not presently attainable due to limits of the gas handling system for the laser; this pressure does not represent a stability limit.

Figure 11 gives typical output spectra of the laser. Spectra are shown for output mirrors of four reflectivities, as indicated on the figure. The rotational and vibrational quantum numbers of the transitions are also given. The system lases on the vibrational bands from $V = 3 \rightarrow 2$ to bands above $V = 15 \rightarrow 14$. The most powerful lasing is on the lower vibrational quantum number bands, $V = 3 \rightarrow 2$ to $V = 7 \rightarrow 6$. These bands possess the shortest wavelength lengths of the output spectrum. Typically, more than 60% of the laser output is on lines of wavelengths below 5.1 microns. It should also be noted that the lines that are lasing have very low rotational quantum numbers, transitions as low as $J = 3 \rightarrow 2$ being observed. This behavior is in marked contrast to a conventional liquid nitrogen cooled CO laser, which produces almost all of its output above 5.1 microns, and which lases on higher rotational lines.

The most power was extracted from the laser with 85% reflectivity mirrors; however, as shown on Fig. 11, the system continued to lase even with a 55% reflecting mirror, at approximately 10% of the power obtained at 85% reflectivity. This is testimony to the high gain of the supersonic flow laser medium.

2.5 Rotational Temperature Measurement

The operating characteristics discussed above, most notably, the very low rotational quantum numbers of the lasing spectral lines, and the evident very high gain of the optical cavity, indicate that the supersonic expansion produces very low in-cavity translational/rotational temperatures. This is

confirmed by a direct measurement of rotational temperature in the nozzle. This measurement was made by monitoring the spontaneous radiative emission emitted from the nozzle by the infrared fundamental vibrational-rotational bands of the CO. For this purpose, CaF_2 windows were installed at nozzle Stations 1, 3, and 4 in the laser (cf. Fig. 2). The windows were carefully designed to preserve a completely flush surface in the nozzle walls.

Most spontaneous radiation measurements were performed at Station No. 3 in the nozzle, with the optical path across the long dimension of the expansion. As can be seen from Fig. 2, the optical path at this station is 10 cm. long. A schematic of the optical setup is shown in Fig. 12. As indicated in the figure, a mirror could be used on the far side of the nozzle from the spectrometer, to reflect emitted radiation back through the test section into the spectrometer. As discussed below, this double pass configuration could be used to measure the integrated absorption coefficients of individual rotational-vibrational lines in the spectrum. Radiation emitted through the window is collected and dispersed by a 1/2 meter Czerny-Turner scanning monochromator, equipped with a 300 line/mm, 4.00 micron blaze, Bausch and Lomb grating. Infrared output was detected by a Davers-type A-10, liquid-nitrogen-cooled InSB detector. The infrared signal was typically chopped at 800 cycles, using a Princeton Applied Research Model 191 mechanical chopper and synchronous motor; the detector output was amplified using a PAR Model 124 phase lock amplifier. The output spectra were recorded on a Varian chart recorder. The relative response of the instrument train, as a function of wavelength, was determined by scanning, at several temperatures, an Infrared Industries Model 464/1018 calibrated blackbody source.

Figure 13 shows a resolved spectrum giving the individual rotational lines of the R-branch of the $V = 1 \rightarrow 0$ band component. As discussed in standard references[14, 15] if $I(J)$ is the peak intensity of the J^{th} rotational line, a plot of $\ln(I\lambda^4/J')$ vs. $J'(J'+1)$ should be linear for an optically thin radiating gas.* Here, λ is the wavelength of the rotational line and

*The intensity must be corrected for any variation of the response of the instrumentation as a function of wavelength.

J' is the rotational quantum number of the upper level in the transition. The slope of such a plot is equal to $B_e\, hc/kT_{ROT}$, where B_e is the rotational constant of the molecule (= 1.93 cm^{-1} for CO), h, c, k are, respectively, Planck's constant, the speed of light, and Boltzmann's constant, and T_{ROT} is the rotational temperature. Hence, the rotational temperature can be determined directly from such a plot.

In the present experiment, the rotational line spectra were obtained using a horizontal optical path along the long dimension of the nozzle at Station No. 3. Further, a mirror was used on the far side of the nozzle from the spectrometer, as shown in Fig. 12. The long optical path was chosen to give adequate intensity to permit resolution of the individual rotational lines. If the gas were optically thin, the use of the reflecting mirror would double the signal received by the spectrometer, neglecting the mirror reflectivity and window transmission losses. However, under the present conditions, the gas is self-absorbing, and considerably less than double the single pass intensity is obtained when the return mirror is used. Assuming the gas conditions are homogeneous across the nozzle, it can be shown[16] that the intensity received at the spectrometer compared to the intensity that would be received for a single pass, optically thin emitter is related to the absorption coefficient by:

$$\frac{I\ (\text{Double pass, self-absorbing})}{I\ (\text{Single pass, optically thin})} = \left\{\sum_{n=0}^{\infty} \frac{(1-P'\chi)^n}{(n+1)!\sqrt{n+1}}\right\}\left\{1-\eta_\omega^2\,\eta_M\right\} + \left\{\sum_{n=0}^{\infty} \frac{(-2P'\chi)^n}{(n+1)!\sqrt{n+1}}\right\}\left\{2\,\eta_\omega^2\,\eta_M\right\} \qquad (1)$$

Here, P' is the absorption coefficient, in cm^{-1}, and χ is the optical path length in cm. η_ω is the transmission of the windows, and η_M is the mirror reflectivity. Note for $\eta_\omega = \eta_M = 1$, $P'\chi \to 0$, this ratio goes to 2.

Figure 14 shows a plot for determination of rotational temperature at Station No. 3 in the nozzle. The mass flow rates and discharge operating conditions are indicated on the figure. $ln\left[\text{CONST.} \times \frac{I\lambda^4}{J'}\right]$ is plotted vs. $J'(J+1)$, both with and without the intensity corrected according to Eq. (1). The self-absorption correction is applied in an iterative fashion.

The rotational temperature is estimated, and the absorption correction calculated from Eq. (1). A new rotational temperature is then inferred from the slope of the corrected points. The iteration is ended when the estimated and inferred temperatures agree within 10%. The procedure is relatively insensitive to the ratio of the populations of the V = 1 and V = 0 vibrational states. The rotational temperature obtained from the slope of the corrected points is 75°K.

3. THEORETICAL MODELLING OF LASER OPERATION

There has been extensive theoretical modelling of kinetic processes in electrically excited CO lasers in the last few years. As part of the present investigation of electrically excited supersonic flow CO lasers, theoretical models and computer codes have been developed to predict performance. A detailed description of these modelling studies is given in Reference 17. As the codes are applied to calculations of the present laser, the following operating conditions must be specified:

i) The mass flow rates of each constituent in the laser.

ii) The inlet temperature of the gases.

iii) The operating pressure in the discharge.

iv) The cross-sectional area of the discharge tube, and the electrode separation in the discharge.

v) The operating voltage and current in the discharge.

vi) The throat area and the expansion angle of the supersonic nozzle.

vii) The location and streamwise extent of the optical cavity.

viii) The mirror reflectivities and losses in the optical cavity.

Given these inputs, the following calculations are performed:

i) A Fokker-Planck type equation governing the electron energy distribution in the discharge is solved. The methods are similar to those published by Nighan.[18] Electron drift velocity, electron number density, and the rate of vibrational excitation of CO molecules by electron impact are calculated.

ii) Equations governing the gas dynamic variables of pressure, temperature, and velocity, together with kinetic equations governing the populations of the individual CO vibrational quantum states, are solved simultaneously for these variables as functions of streamwise position.

iii) Output power from the flow laser is calculated using a Fabry-Perot cavity (flat-flat mirrors) model, having an optical axis perpendicular to the flow direction. With this approximation, a quasi-one-dimensional flow calculation for the gasdynamics and CO kinetics provides a consistent description of the coupling between these processes and the radiation field. A solution to this problem has all the essential coupling features but not the complexity of a curved mirror system. For this cavity model, the calculation of the gasdynamic properties, vibrational level populations, and lasing intensities in a CO flow laser is like that used for chemical lasers by Emanuel.[19]

The equations that are solved are one-dimensional; distance in the flow direction is the only independent variable; variation of medium properties normal to the flow direction is neglected. The kinetic processes controlling the CO vibrational state populations included in the model are collisionally induced exchange of energy between the modes of CO vibration and heavy species translational and rotational motion; exchange between vibration and electron motion; vibration-to-vibration energy exchange among colliding CO molecules; and spontaneous radiative decay. References 6-10 and 17 discuss the influence of these kinetic processes in detail.

Figures 15 and 16 show the calculated results for typical room temperature operation of the electrically excited supersonic flow laser. In Fig. 15, the variation of temperature, pressure, and vibrational energy through the laser is plotted. The operating conditions are as indicated on the figure. The gradual rise in power in the vibrational mode of the CO, as the gas is processed by the discharge, can be observed. An increase in translational temperature is also observed. These calculations indicate approximately 25% of the total electrical power goes into the CO vibrational mode. Very little of this vibrational mode power is lost as the gas is expanded in the nozzle. Typical measured temperature and pressures in the nozzle expansion are also shown. It should be noted that the expansion ratio

of the nozzle in the calculated results was chosen to match the observed pressure distribution, i.e., the calculation is for the effective expansion ratio of the nozzle, not for the geometrical expansion.

On the basis of the preceding correlation of the theoretical model with measurements, a temperature of 40°K in the optical cavity at Station No. (1) (Fig. 2) is inferred. Figure 16 shows the spectral power distribution for the optical cavity at Station No. (1) ($A/A_{throat} = 8.9$) compared with the experimentally measured laser spectrum. It is seen that the spectral distributions are in approximate agreement; the theoretically predicted spectra show somewhat greater weighting of intensities at short wavelengths. This shift can perhaps be attributed to the experimental cavity being slightly warmer than the theoretically predicted 40°K. However, it is noteworthy that the peak gain rotational lines predicted coincide with those measured; these are the P(3) to P(6) lines in each band.

4. SUMMARY AND CONCLUSIONS

The present electrically excited supersonic flow CO laser has been operated at power levels of ~350 watts c.w., at 12% efficiency and specific powers of 14.5 kw/lb/sec. For these operating conditions, the discharge pressure is 684 torr, and the in-cavity pressure is 2.5 torr. A correlation of theoretical calculation with measurements of rotational temperature in the nozzle expansion indicate an in-cavity temperature of 40°K. More than 60% of the output power is distributed among approximately 15 lines at wavelengths from 4.819 to 5.084 microns; the remaining power occurs on lines from 5.132 microns to above 5.758 microns.

Some principal findings of the present study are:

i) It is possible to operate a stable axial flow glow discharge in a CO/He plasma at pressures of at least 1.5 atmospheres.

ii) Use of electrical excitation and supersonic flow to obtain low in-cavity temperatures results in a powerful and efficient CO laser producing more than 60% of its output at wavelengths below 5.1 μ.

iii) Lasing action has been obtained on many vibrational-rotational spectrum lines of CO with extremely low J values; these have not previously been identified in CO laser emission.

TABLE 1

HIGH PRESSURE OPERATION OF THE ELECTRICALLY EXCITED SUPERSONIC FLOW CARBON MONOXIDE LASER

RUN NO.	PLENUM PRESSURE, atm	INLET GAS TEMPERATURE, °K	MASS FLOW OF He, lb/sec^{-1}	MASS FLOW OF CO, lb/sec^{-1}	MOLE FRACTION OF CO, %	LASER POWER, watts	MASS EFFICIENCY, kW/lb/sec	ELECTRICAL EFFICIENCY, %	DISCHARGE VOLTAGE, kV	DISCHARGE CURRENT, mA
1	1.5	300	.0317	.0045	1.99	290	8.01	9.1	40	80
2	1.5	300	.0308	.0073	3.26	350	9.17	10.4	48	70
3	1.5	200	.0312	.0055	2.44	300	8.17	11.0	44	62

REFERENCES

1. Osgood, R. M., Jr., Eppers, W. C., Jr., and Nichols, E. R., IEEE J. Quantum Electron Q. E. -6, 145, 1970.

2. Nighan, W. L., Appl. Phys. Lett. 20, 96, 1972.

3. Rich, J. W., Watt, W. S., and Thompson, H. M., U. S. Air Force Avionics Laboratory Technical Report AFAL-TR-71-152, March 1971.

4. Bhaumik, M. L., Lacina, W. B., and Mann, M. M., IEEE J. Quantum Electron Q. E. -6, 575, 1970.

5. Rich, J. W., Thompson, H. M., Treanor, C. E., and Daiber, J. W., Appl. Phys. Lett. 19, 230, 1971.

6. Treanor, C. E., Rich, J. W., and Rehm, R. G., J. Chem. Phys. 48, 1798, 1968.

7. Bray, K. N. C., J. Phys. B. (London) Ser. 2, 1, 705, 1968; 3, 1515, 1970.

8. McKenzie, R. L., Technical Report No. NASA TN-D-7050, March 1971.

9. Rich, J. W., J. Appl. Phys. 42, 2719, 1971.

10. Center, R. E. and Caledonia, G. E., Appl. Optics 10, 1795, 1971; J. Chem. Phys. 55, 552, 1971.

11. McKenzie, R. L., Appl. Phys. Lett. 17, 462, 1970.

12. Watt, W. S., Appl. Phys. Lett. 18, 487, 1971.

13. Gibbs, W. E. K. and McLeary, R., Phys. Letters 37A, 229, 1971; McLeary, R. and Gibbs, W. E. K., IEEE J. Quantum Electron Q. E. -9, 828, 1973.

14. Herzberg, G., Spectra of Diatomic Molecules, 2nd Ed., p. 129, Van Nostrand Princeton, New Jersey, 1950.

15. Penner, S. S., Quantitative Molecular Spectroscopy and Gas Emissivities, Chap. 17. Addison-Wesley, Reading, Massachusetts, 1959.

16. Rich, J. W., Bergman, R. C., Thompson, H. M., and Lordi, J. A., U. S. Air Force Avionics Laboratory Technical Report AFAL-TR-73-294, September 1973.

17. Rich, J. W., Lordi, J. A., and Kang, S. W., Calspan Corporation Report WG-5164-A-1, December 1972.

18. Nighan, W. L., Appl. Phys. Lett. 20, 99, 1972.

19. Emanuel, G., "RESALE-1: A Chemical Laser Computer Program," Aerospace Corporation Report TR-D172(2776)-1, March 1972.

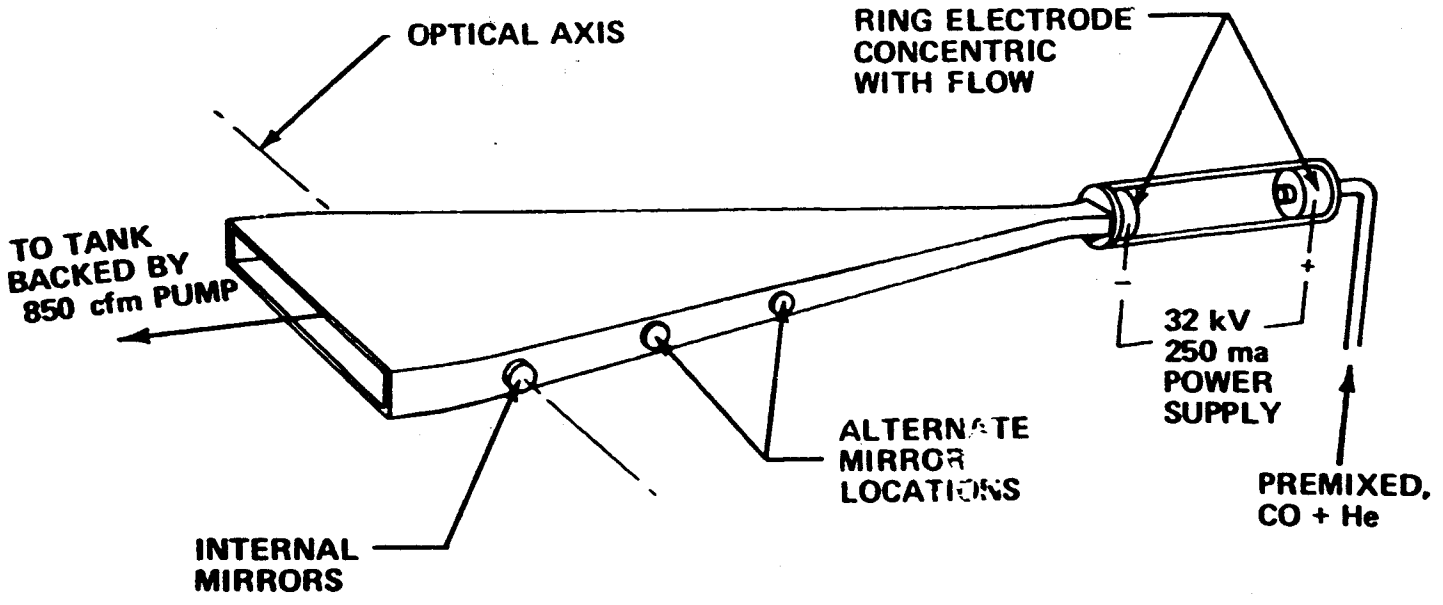

Figure 1 PERSPECTIVE SKETCH OF THE ELECTRICALLY EXCITED SUPERSONIC FLOW CO LASER

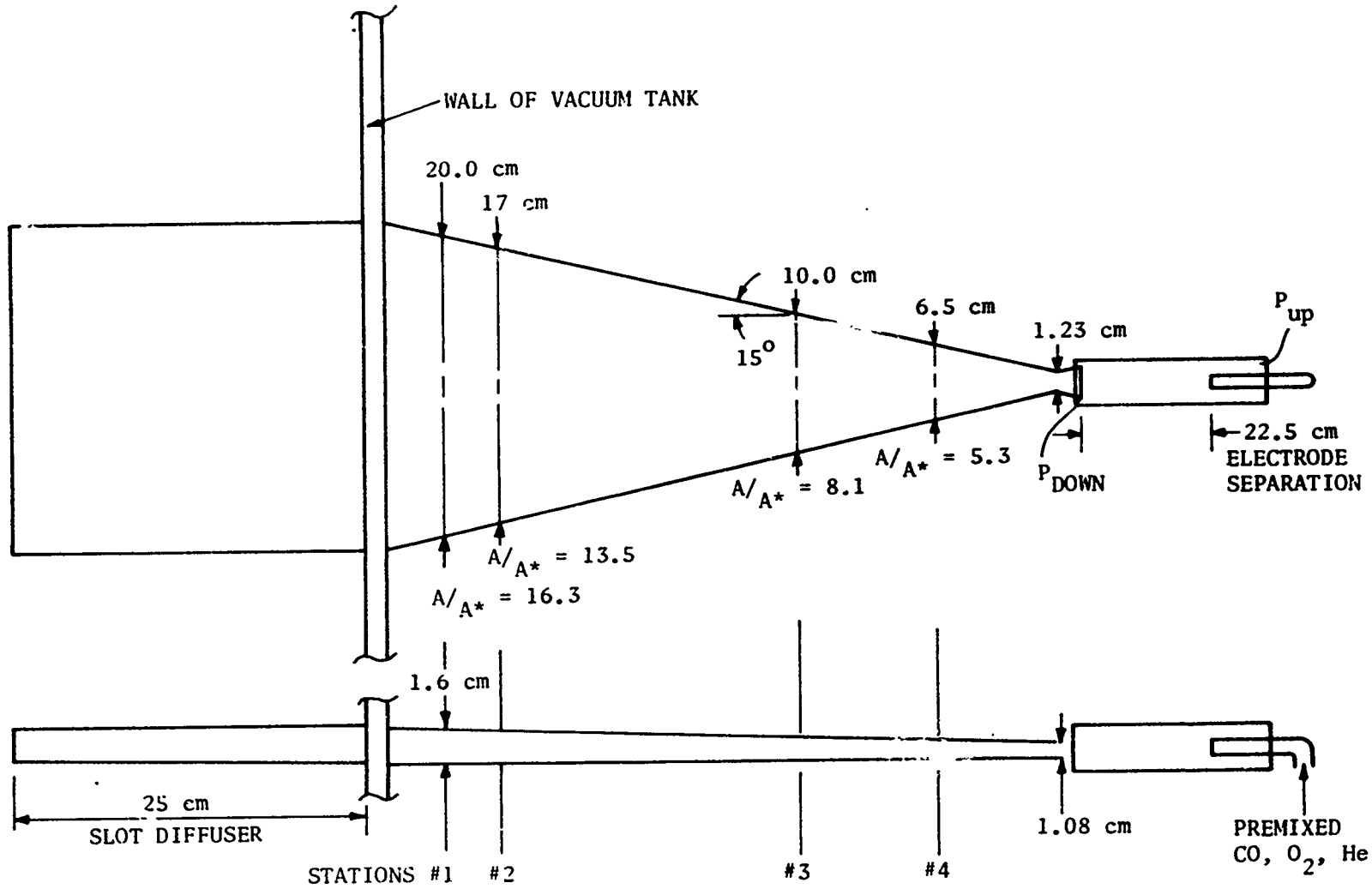

Figure 2 **SCHEMATIC DIAGRAM OF THE ELECTRICALLY-EXCITED SUPERSONIC FLOW CO LASER**

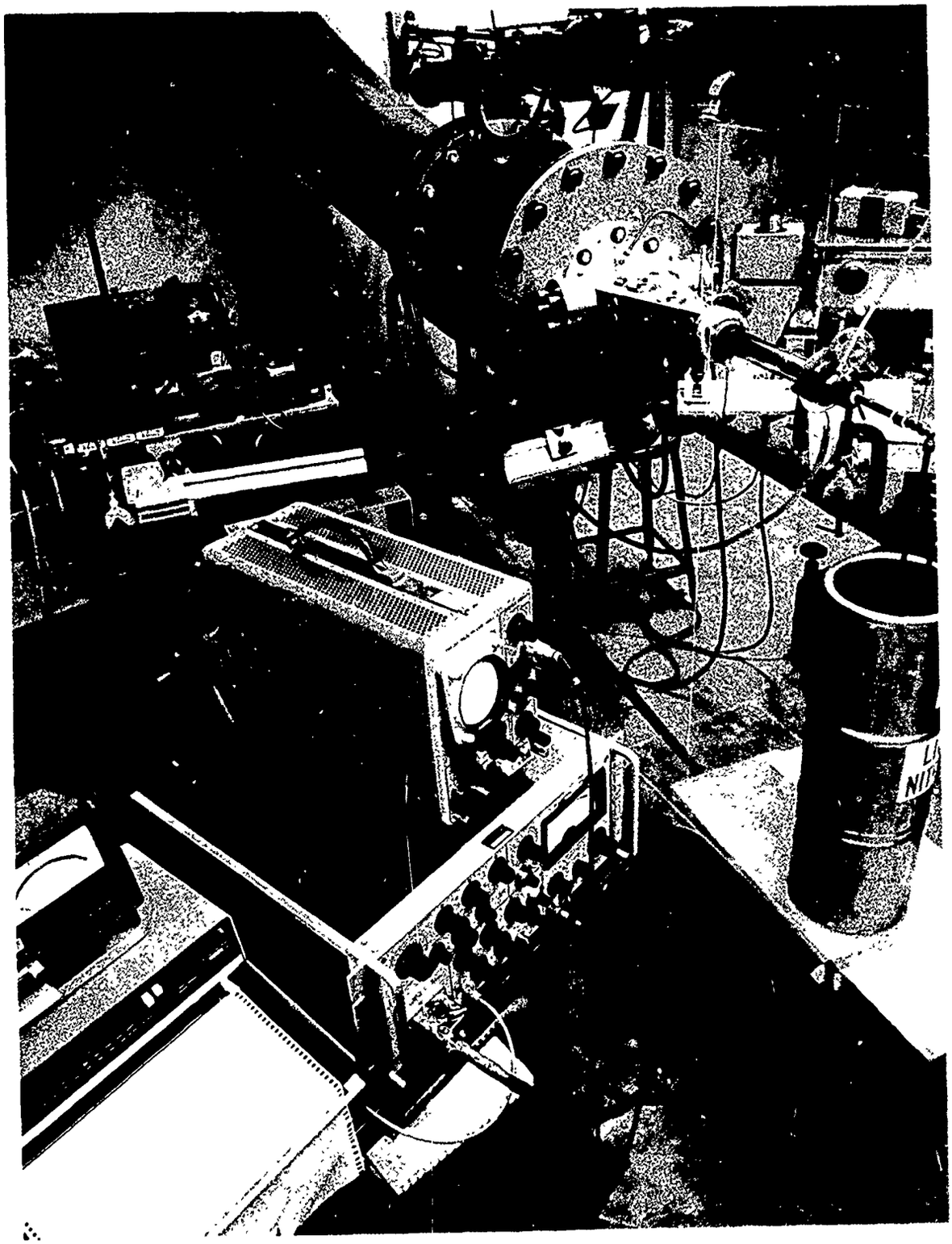

Figure 3 SUPERSONIC FLOW CO LASER LABORATORY

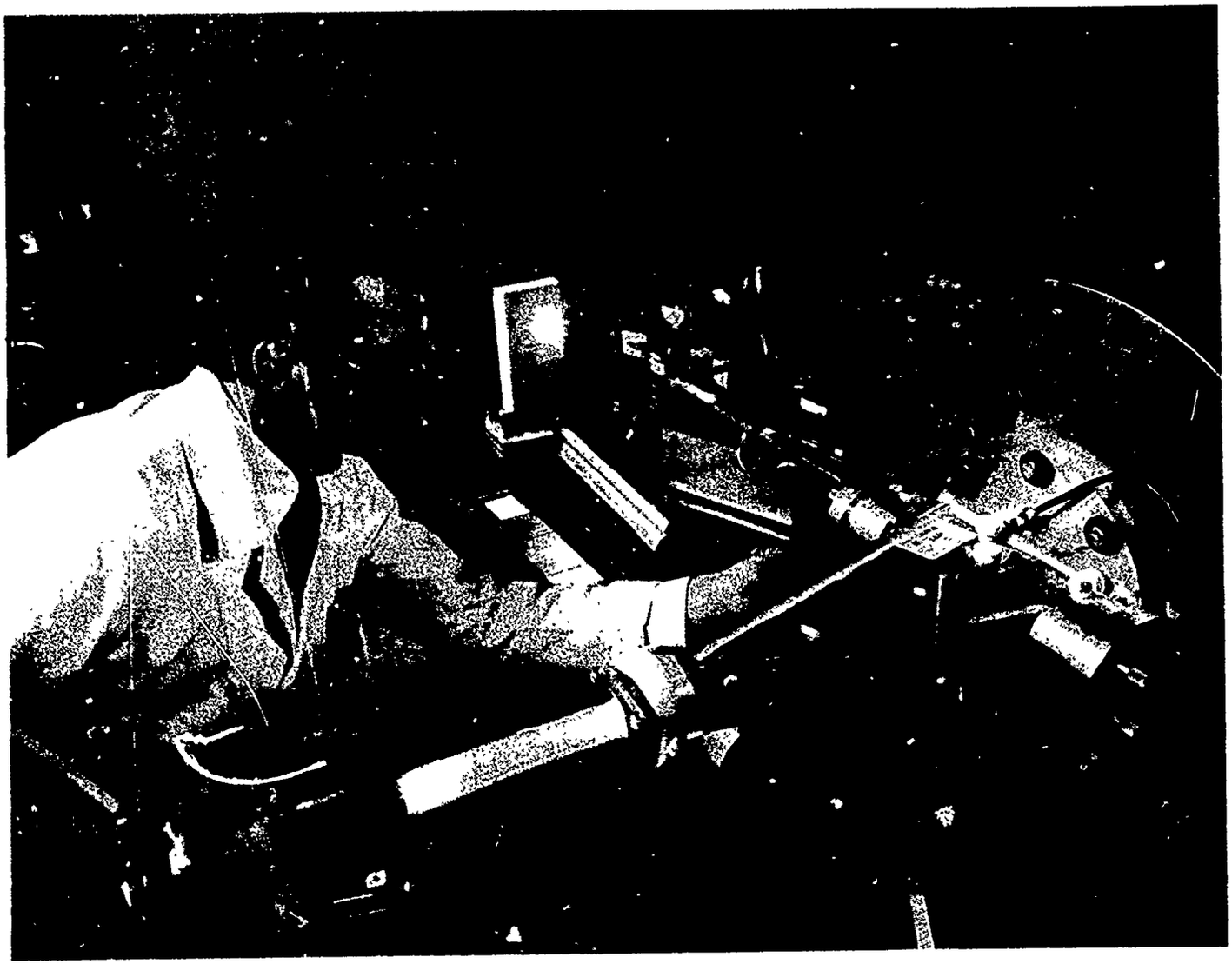

Figure 4 SUPERSONIC FLOW CO LASER IN OPERATION

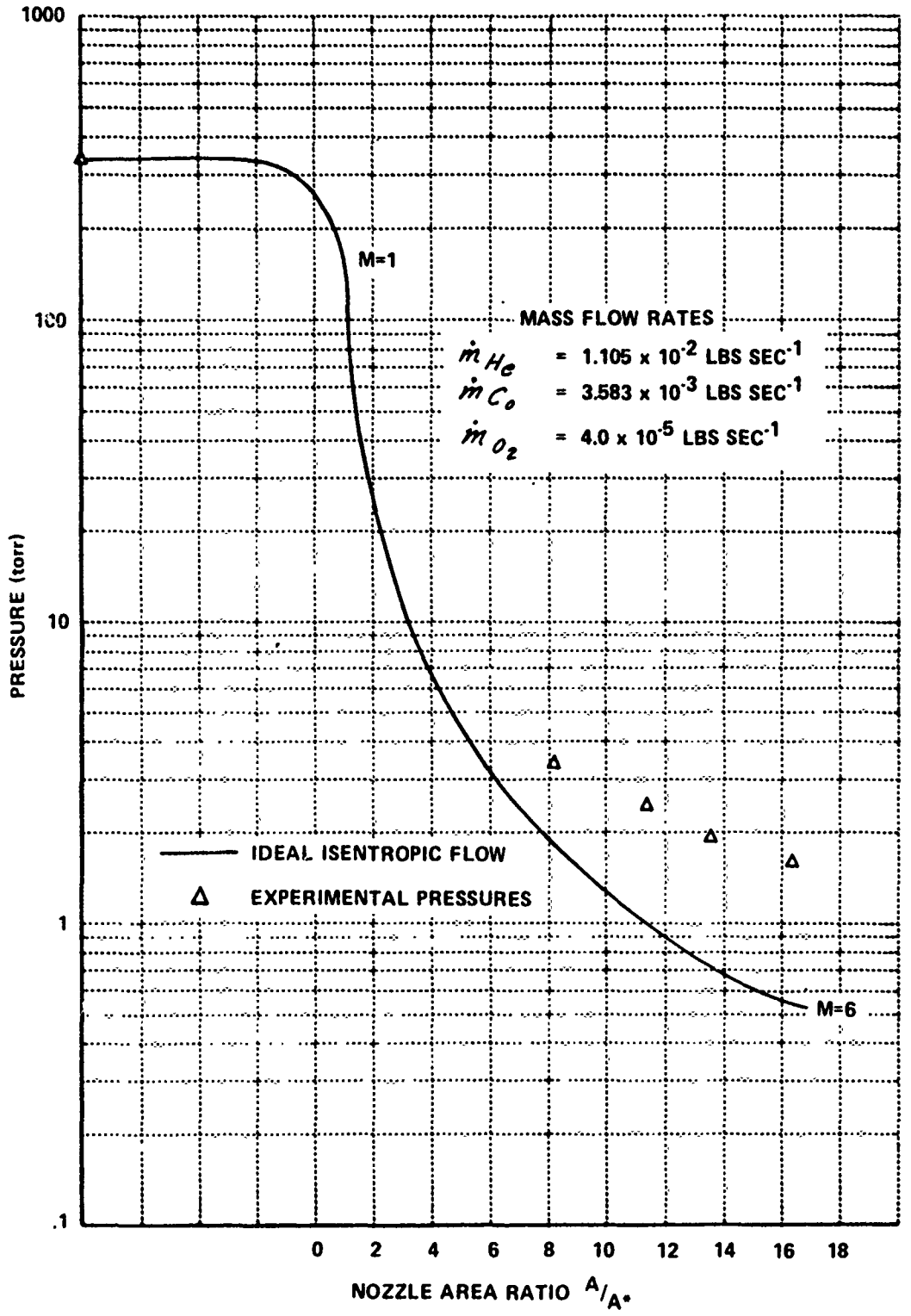

Figure 5 STATIC PRESSURE DISTRIBUTION IN THE LASER

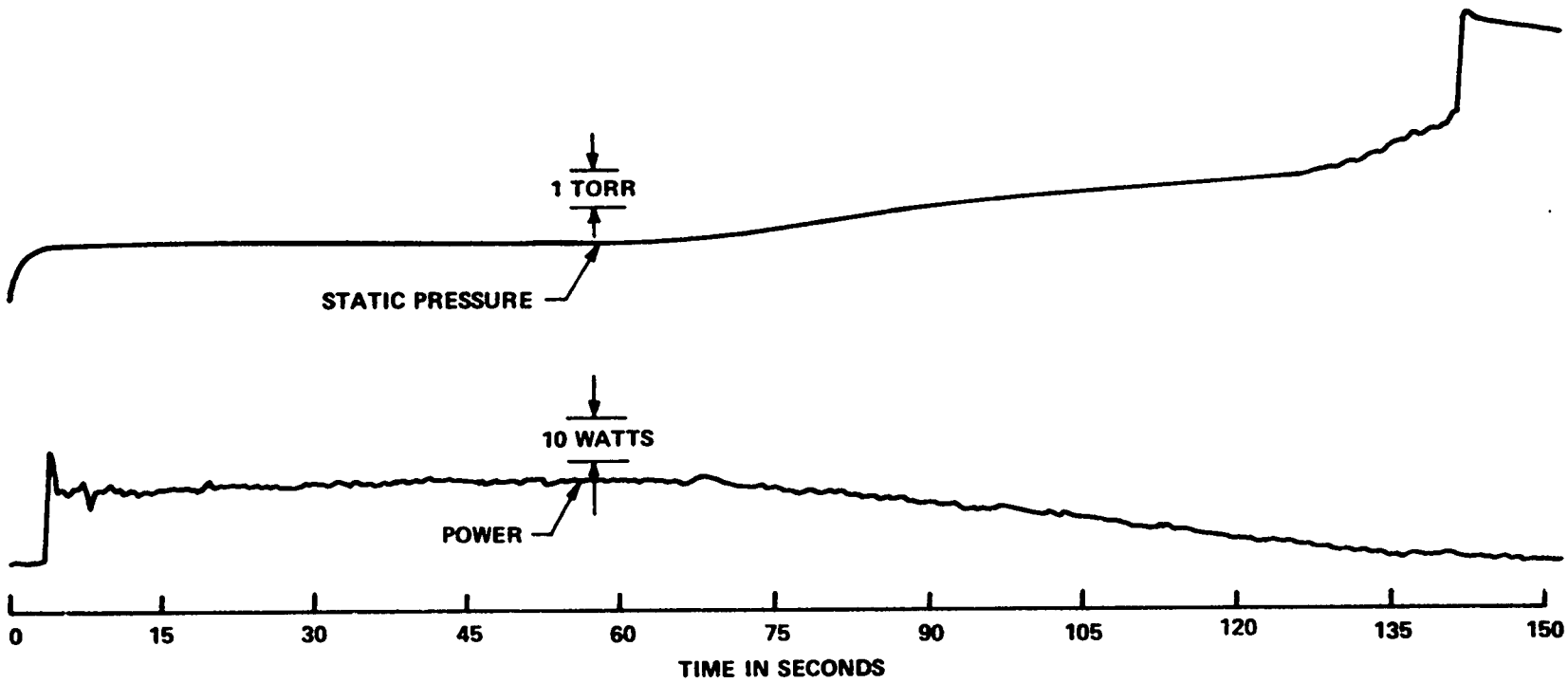

Figure 6 POWER AND PRESSURE HISTORIES DURING A SINGLE RUN PERIOD

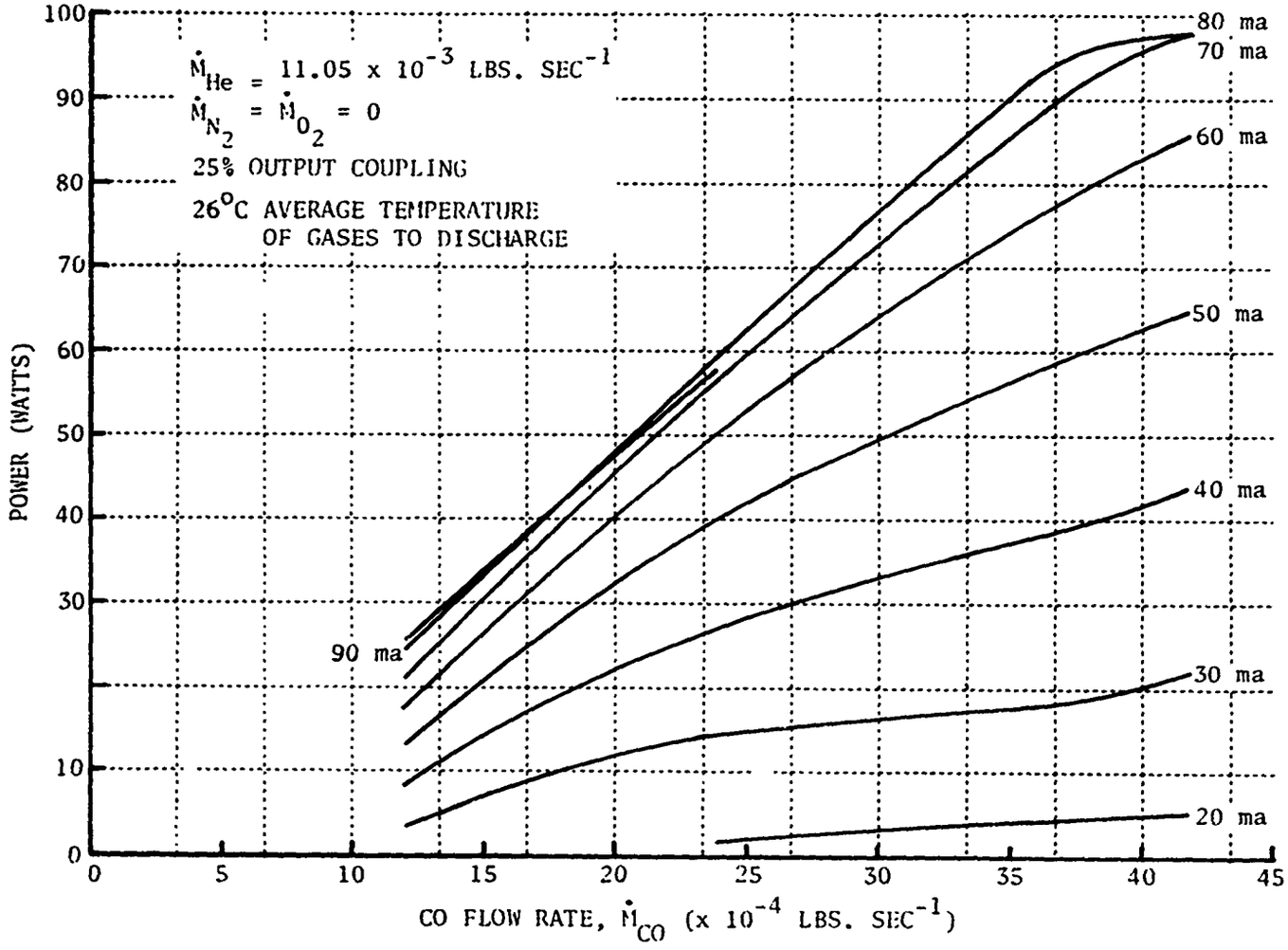

Figure 7 POWER VS CO FLOW RATE, ROOM TEMPERATURE OPERATION

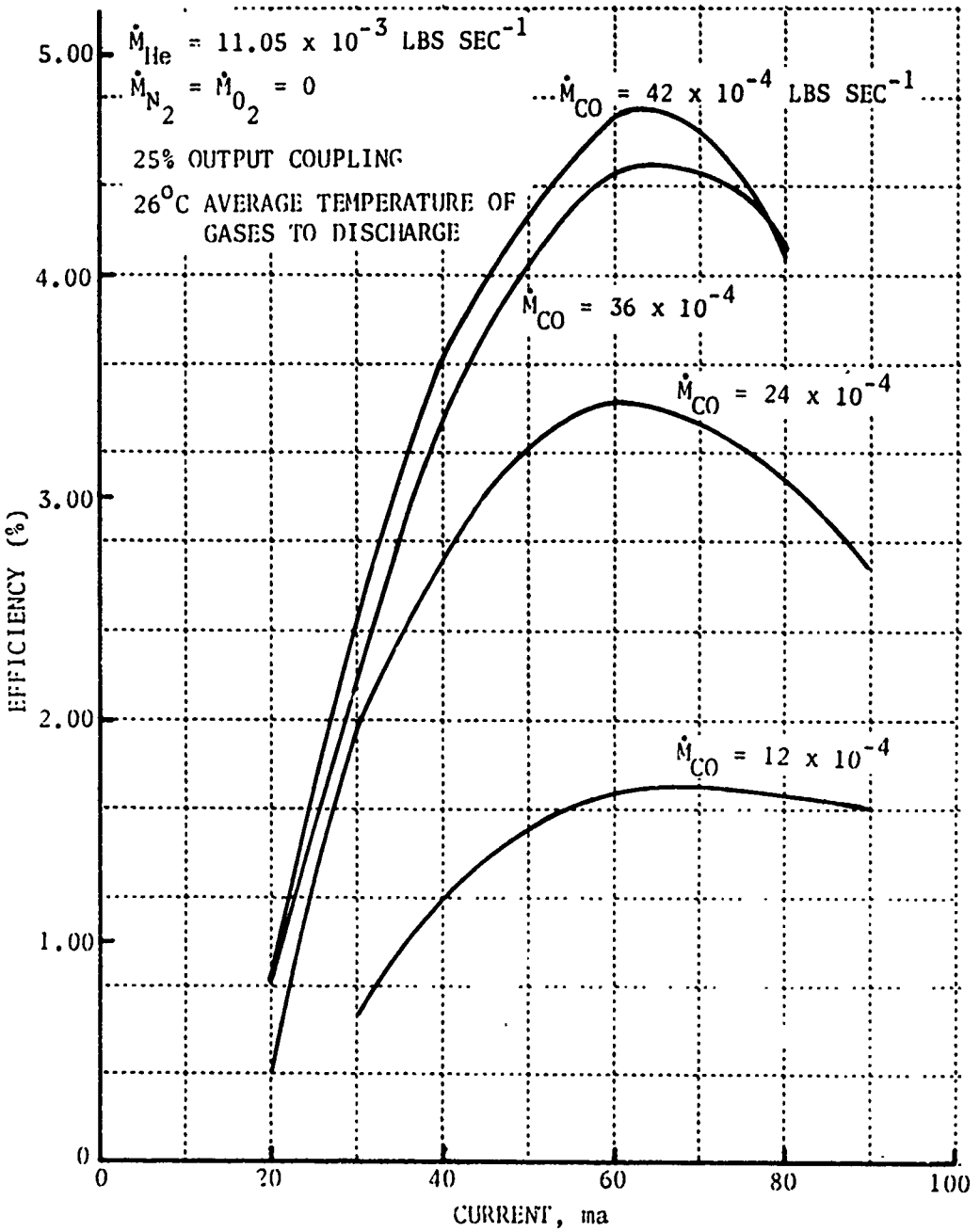

Figure 8 EFFICIENCY VS CURRENT, ROOM TEMPERATURE OPERATION

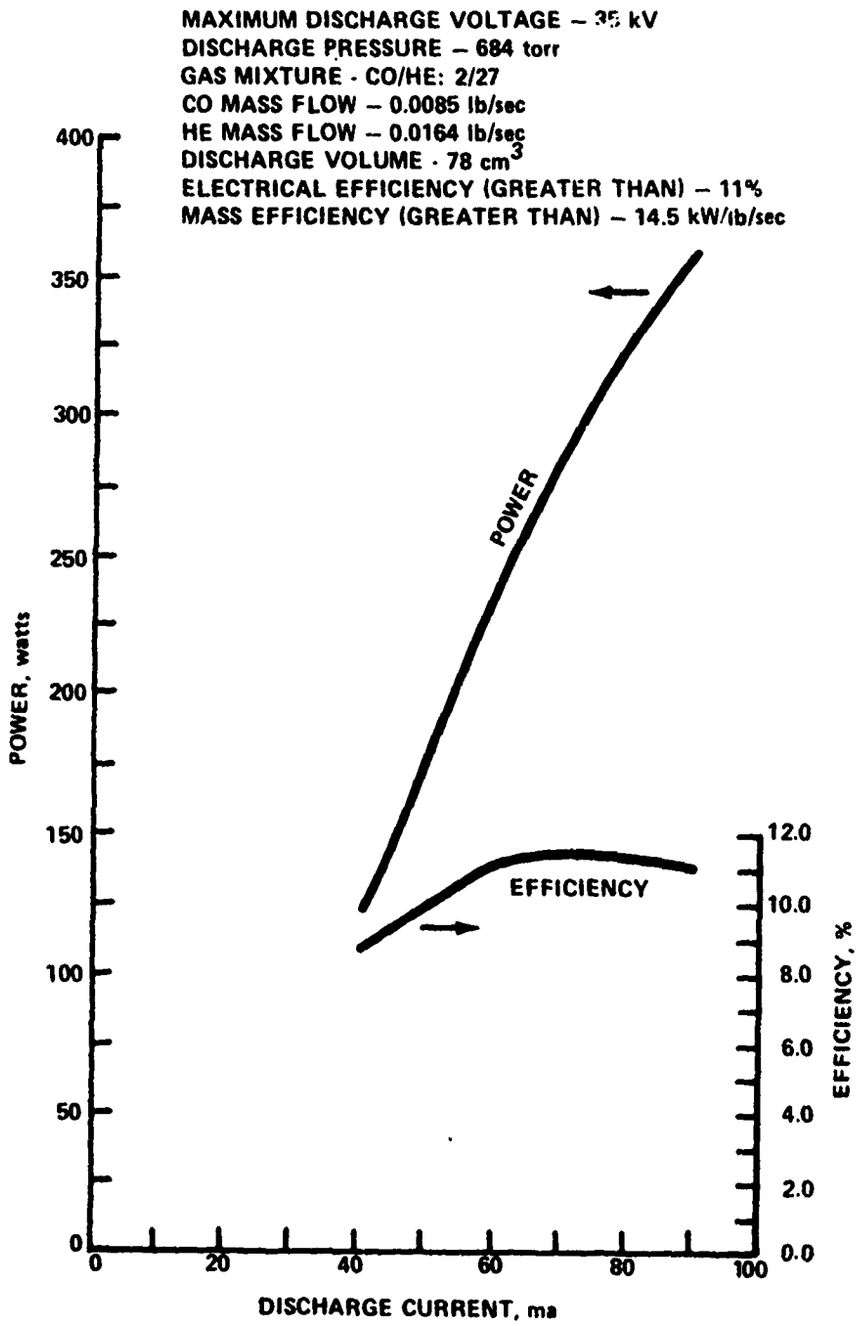

Figure 9 CO SUPERSONIC LASER PERFORMANCE AT HIGH DISCHARGE PRESSURE

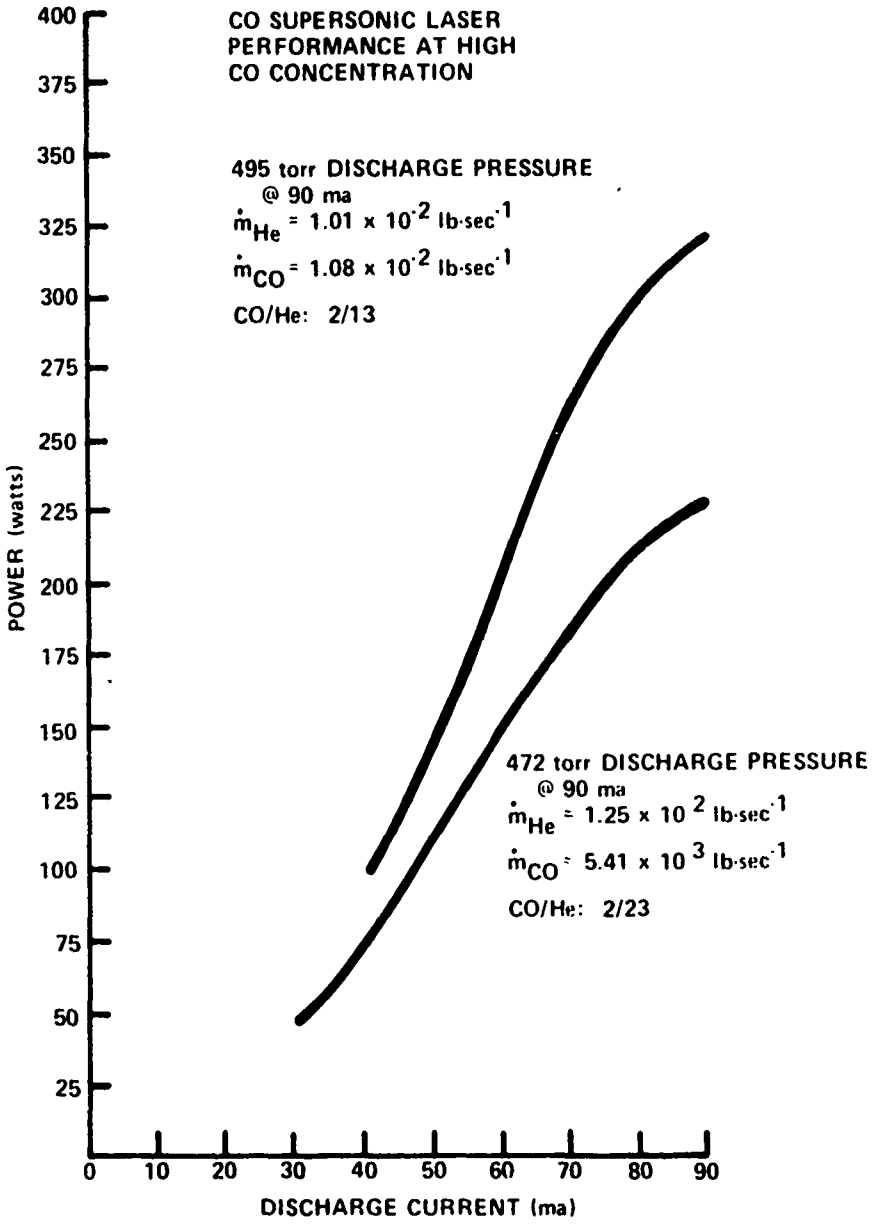

Figure 10 CO SUPERSONIC LASER PERFORMANCE AT HIGH CO CONCENTRATION

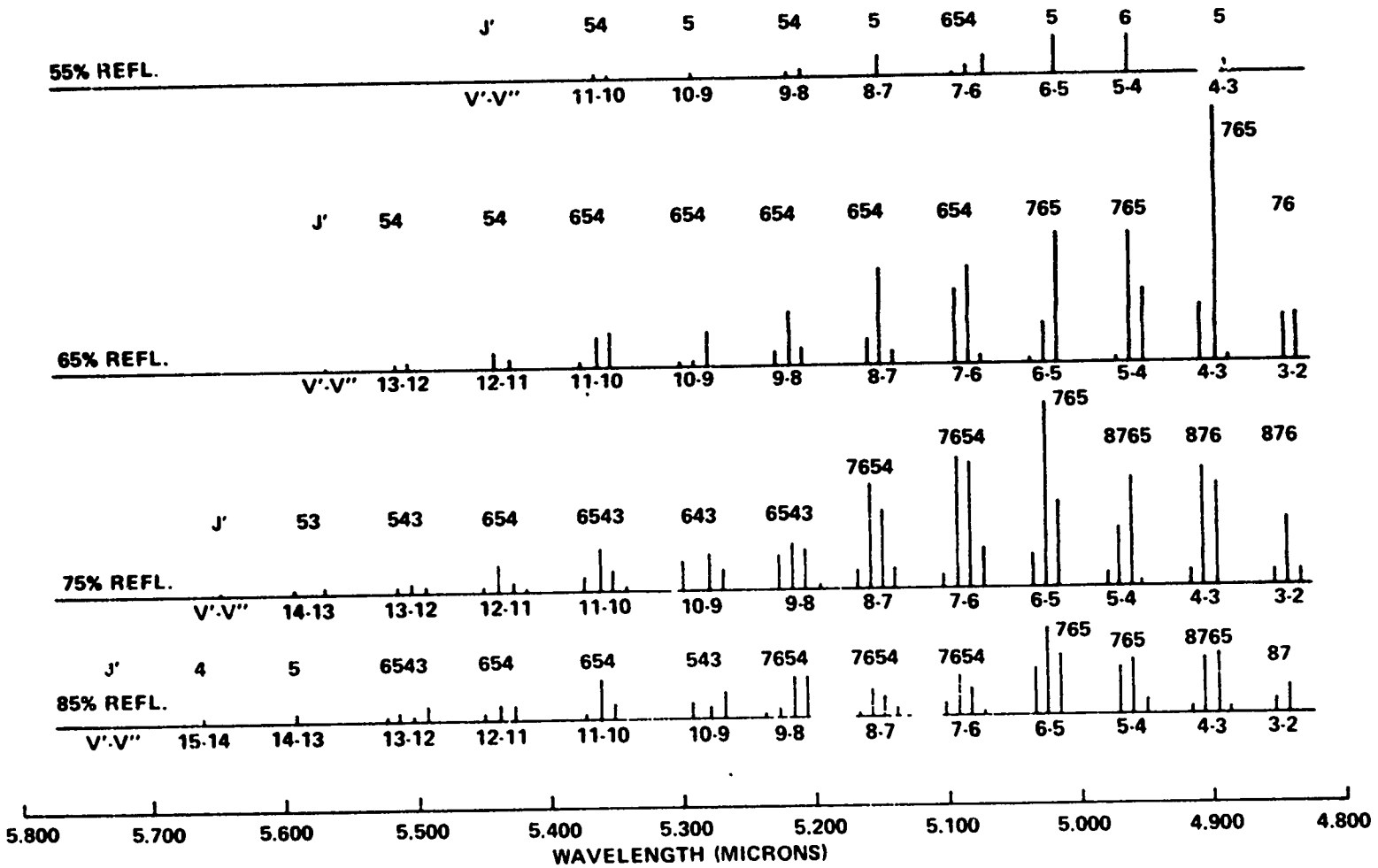

Figure 11 CO LASER SPECTRA AT VARIOUS OUTPUT COUPLINGS, ROOM TEMPERATURE OPERATION

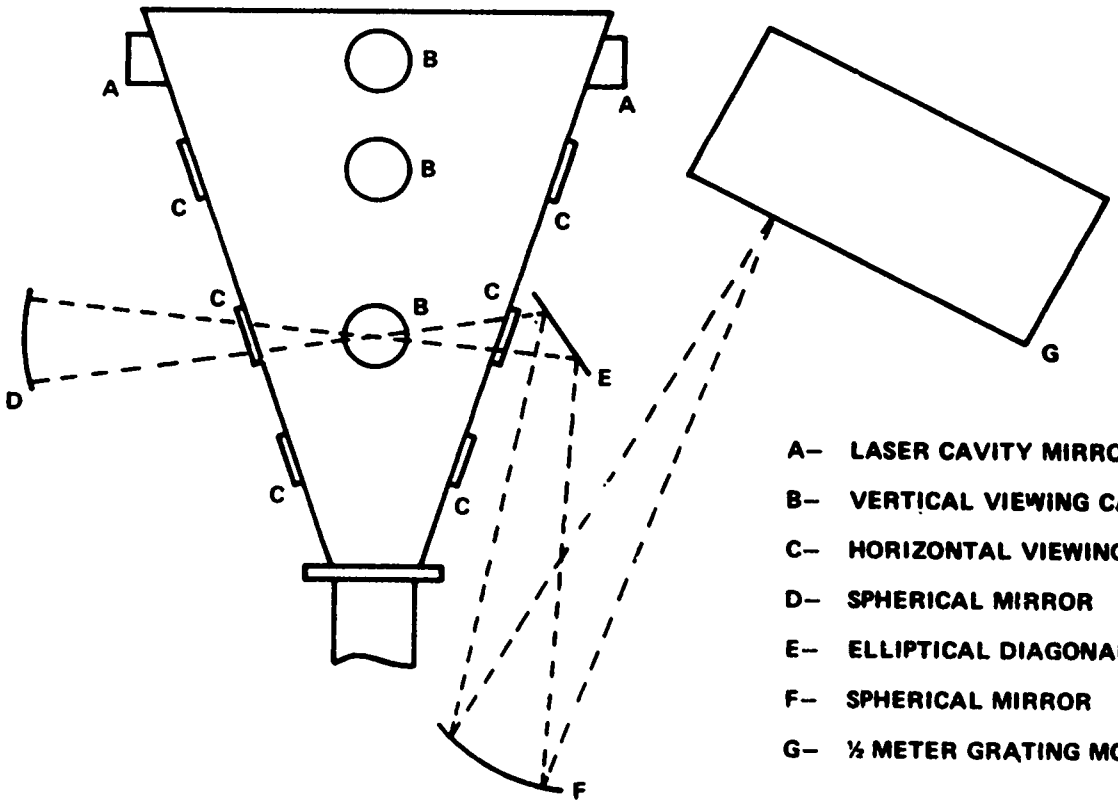

A– LASER CAVITY MIRROR MOUNTS

B– VERTICAL VIEWING CALCIUM FLUORIDE WINDOWS

C– HORIZONTAL VIEWING CALCIUM FLUORIDE WINDOWS

D– SPHERICAL MIRROR

E– ELLIPTICAL DIAGONAL MIRROR

F– SPHERICAL MIRROR

G– ½ METER GRATING MONOCHROMATOR

Figure 12 INFRARED SIDELIGHT EXPERIMENT - SCHEMATIC

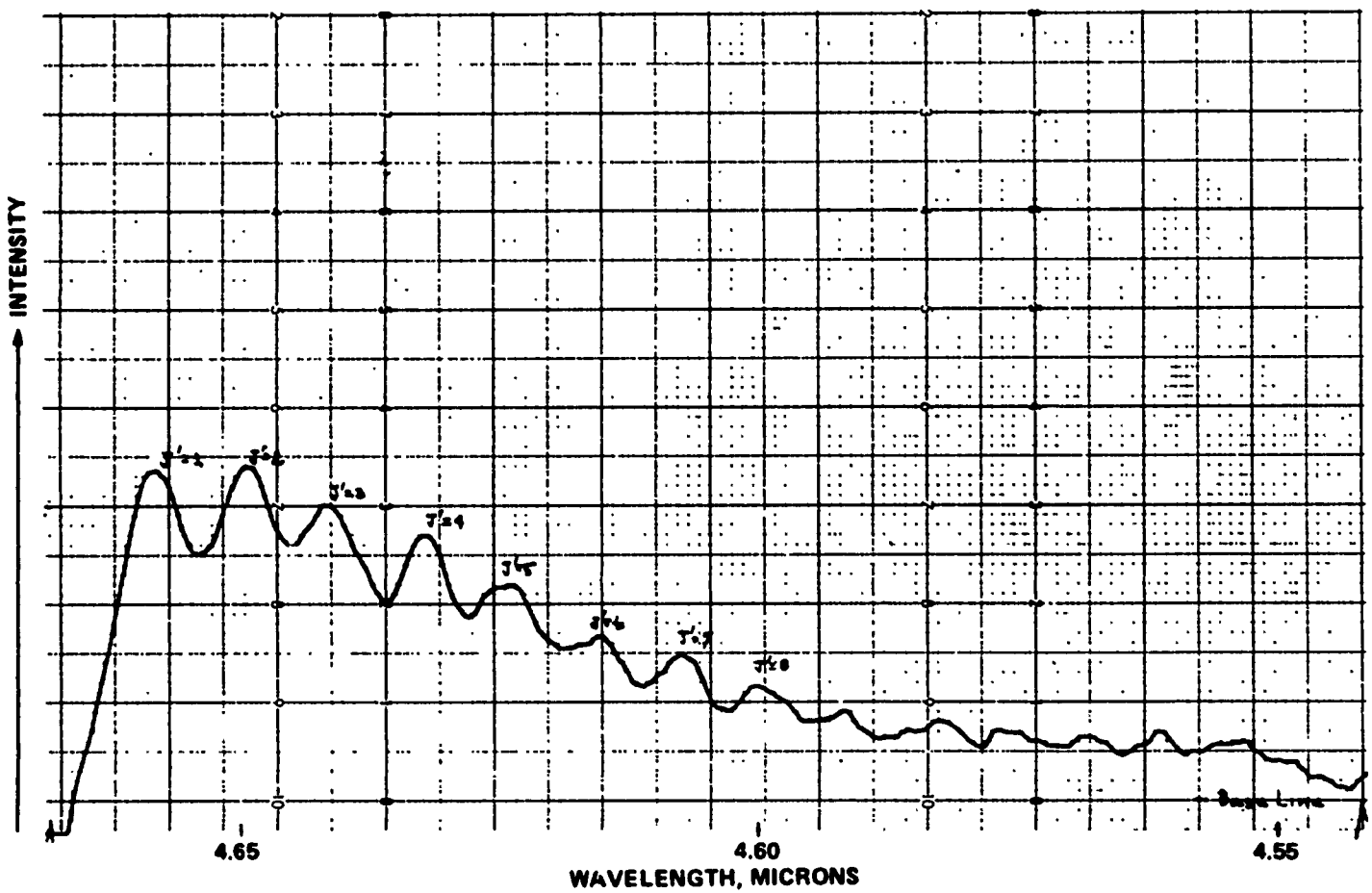

Figure 13 SIDELIGHT EMISSION SPECTRUM - RESOLUTION OF ROTATIONAL LINES

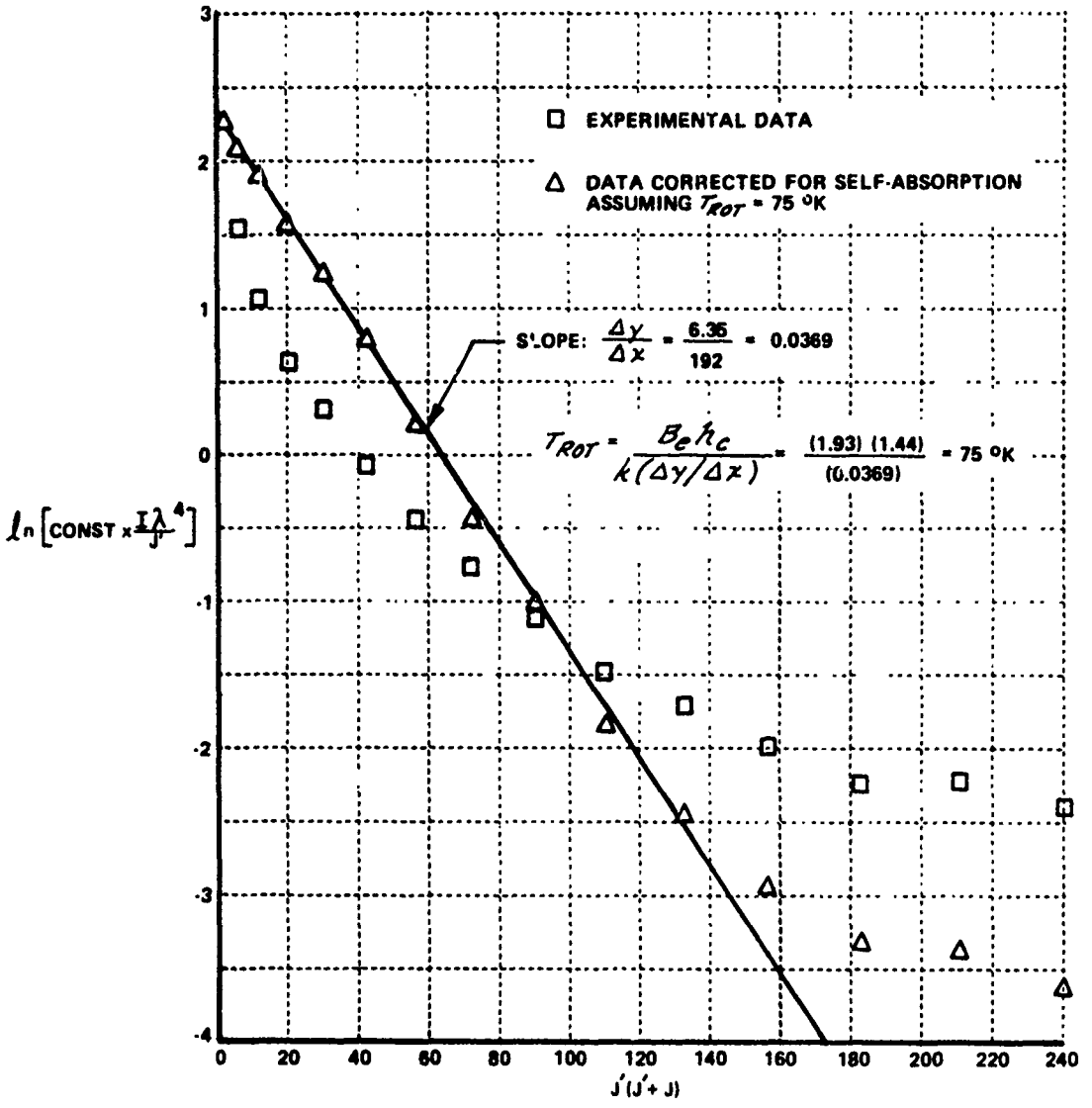

29.0 kv DISCHARGE VOLTAGE
70.0 ma DISCHARGE CURRENT
40 watts POWER OUTPUT
372 torr TOTAL DISCHARGE PRESS.
3.8 torr NSP AT STATION NO. 4
18 °C TEMP. INLET GASES
$\dot{m}_{CO}$ = 35.83×10^{-4} lbs sec^{-1}
$\dot{m}_{He}$ = 11.05×10^{-3} lbs sec^{-1}

Figure 14 DETERMINATION OF ROTATIONAL TEMPERATURE

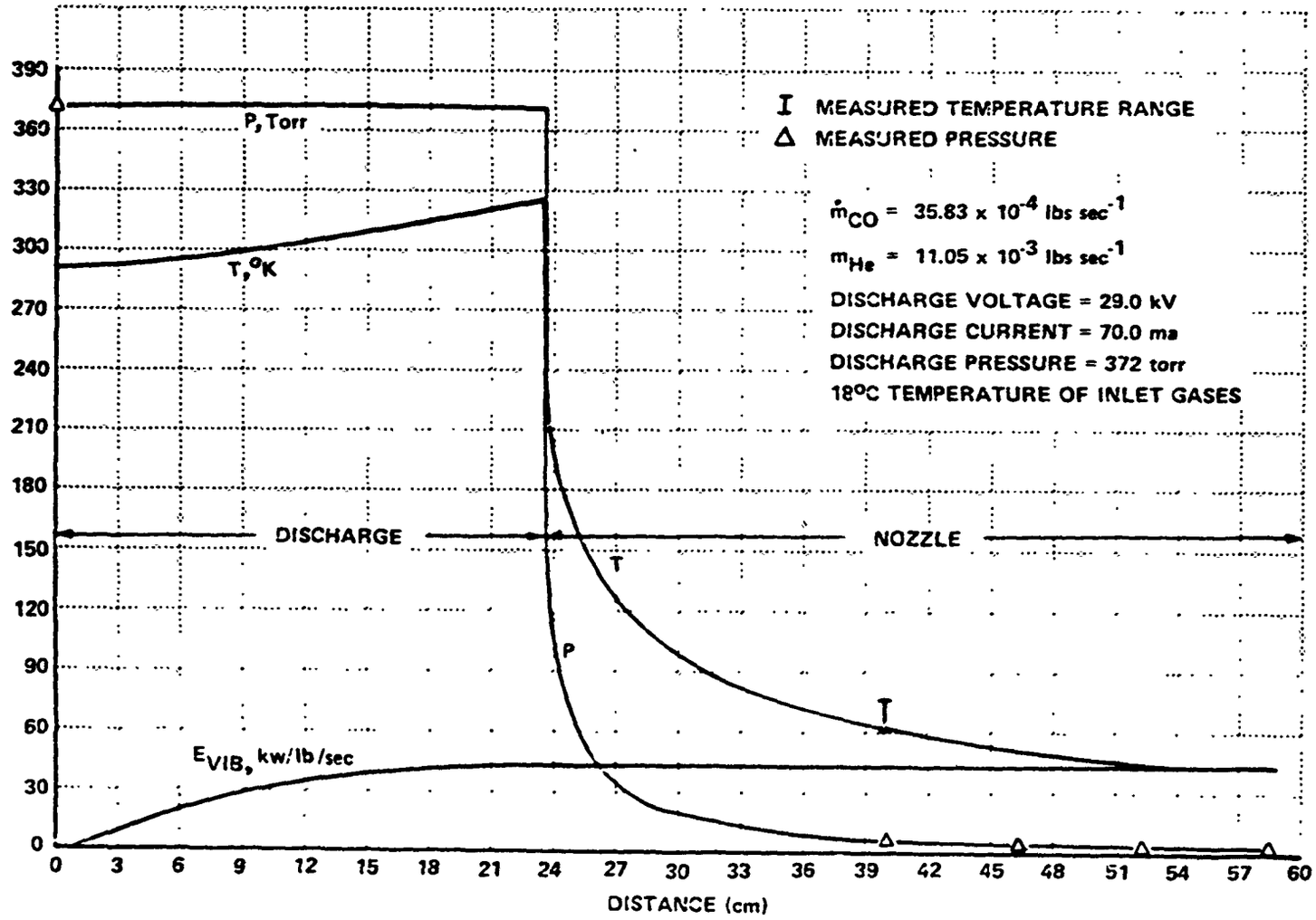

Figure 15 PREDICTED PRESSURE, TEMPERATURE, AND VIBRATIONAL ENERGY IN THE PROTOTYPE CO SUPERSONIC FLOW LASER

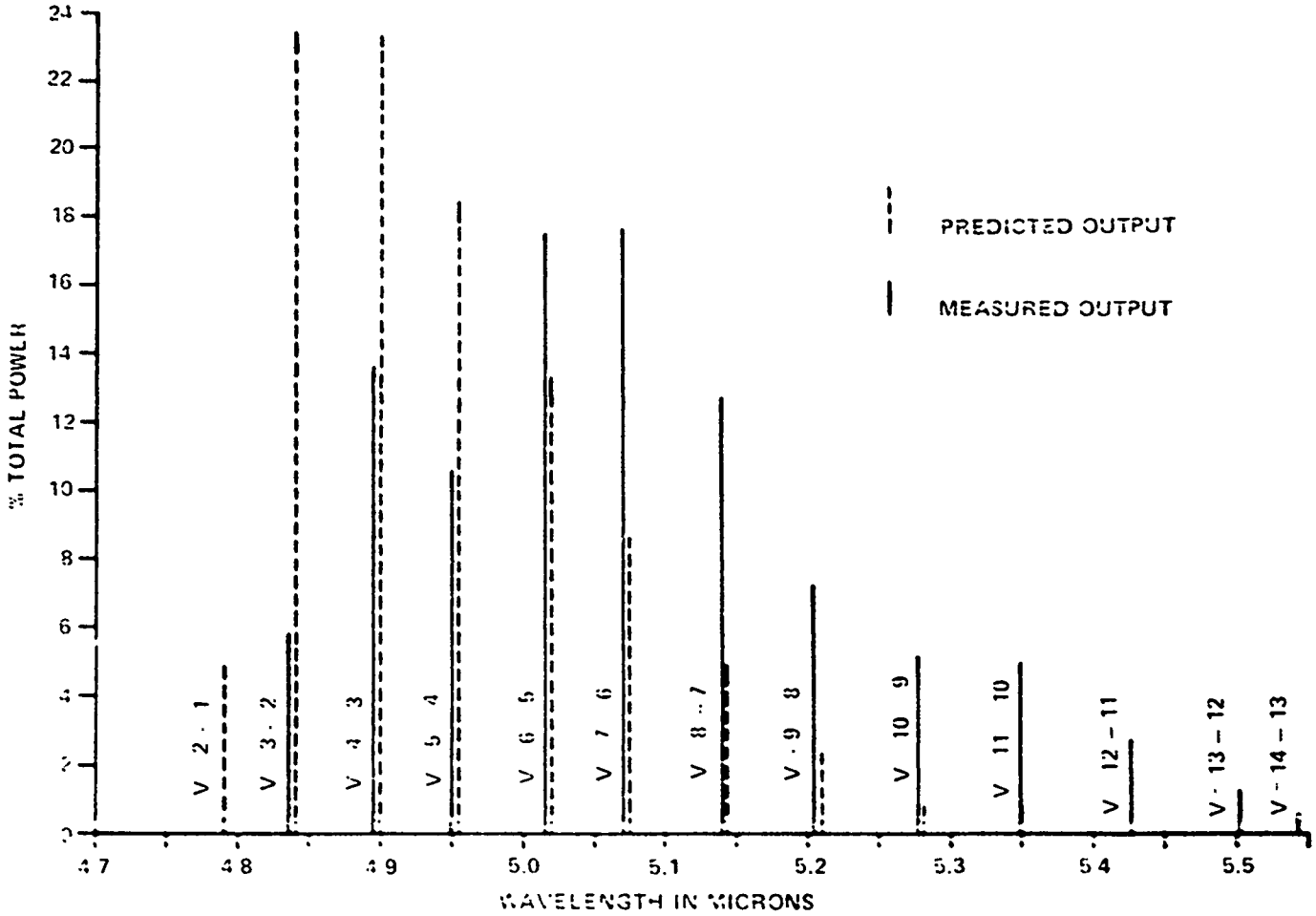

Figure 16 COMPARISON OF PREDICTED AND MEASURED OUTPUT IN THE PROTOTYPE CO SUPERSONIC LASER

REFERENCES

1. Rich, J.W., Bergman, R.C., and Lordi, J.A., Paper No. 74-179, presented at AIAA 12th Aerospace Science Meeting, Washington, D.C., January 30 - February 1, 1974; to be published, AIAA Journal.

2. Rich, J.W., Bergman, R.C., Thompson, H.M., and Lordi, J.A., U.S. Air Force Avionics Laboratory Report AFAL-TR-73-294, September 1973.

3. Rich, J.W., Thompson, H.M., Treanor, C.E., and Daiber, J.W., Appl. Phys. Lett. 19, 230 (1971).

4. McLeary, R. and Gibbs, W.E.K., IEEE J. Quant. Electronics, QE-9, 828 (1973).

5. McLeary, R. and Gibbs, W.E.K., Report 486, Dept. of Supply Australian Defence Scientific Service, Defence Standards Laboratories, Maribyruong, Victoria, Australia, December 1971.

6. Gibbs, W.E.K. and McLeary, R., Phys. Lett. 37A, 229 (1971).

7. McKenzie, R.L., Appl. Phys. Lett. 17, 462 (1970).

8. Watt, W.S., Appl. Phys. Lett. 18, 487 (1971).

9. Osgood, R.M., Jr., Eppers, W.C., Jr., and Nichols, E.R., IEEE J. Quantum Electron QE-6, 145 (1970).

10. McClatchey, R.A., "Atmospheric Attenuation of CO Laser Radiation", Cambridge Research Laboratories Technical Report AFCRL-71-0370, 1 July 1971; McClatchey, R.A., private communication.

11. Brunet, H., private communication.

12. Rich, J. W., Watt, W. S., and Thompson, H. M., U. S. Air Force Avionics Laboratory Report AFAL-TR-71-152, March 1971.

☆U.S.Government Printing Office: 1975 — 657-022/605